INTERNATIONAL ATOMIC ENERGY AGENCY
UNITED NATIONS EDUCATIONAL, SCIENTIFIC AND CULTURAL ORGANIZATION

INTERNATIONAL CENTRE FOR THEORETICAL PHYSICS
34100 TRIESTE (ITALY) - P.O.B. 586 - MIRAMARE - STRADA COSTIERA 11 - TELEPHONES: 224281/2/3/4/5/6
CABLE: CENTRATOM - TELEX 460392-1

SMR/100 - 26

WINTER COLLEGE ON LASERS, ATOMIC AND MOLECULAR PHYSICS

(24 January - 25 March 1983)

Spectroscopy and Structure of the Hydrogen Molecular Ion

A. CARRINGTON

Department of Chemistry
University of Southampton
Southampton SO9 5NH
U.K.

by A. [illegible] and [illegible]

(Department of Chemistry, University of Southampton, England)

I. INTRODUCTION

The hydrogen molecular ion, H_2^+, and its isotopic relations HD^+ and D_2^+ have occupied an important position in the development of molecular quantum mechanics since the foundations of the subject some sixty years ago. Many different approximations and methods have been tested on H_2^+ as a model system and it is, of course, the molecule for which the most accurate calculations can be performed, essentially because of the absence of inter-electron interactions. H_2^+ is, however, rather more amenable to theoretical than to experimental investigation. There are two main reasons for this, chemical and structural. The first difficulty is that H_2^+ reacts extremely rapidly with molecular hydrogen to form the H_3^+ ion; electrical discharges in H_2, for example, lead to extensive ionisation but unless the gas pressure is extremely low, H_3^+ is the predominant ionic species present. This fact has been used recently to advantage by Oka [1] and by Carrington, Buttenshaw and Kennedy [2] in their spectroscopic investigations of H_3^+. As we shall see, however, spectroscopic studies of H_2^+ have necessarily made use of collision-free media. H_2^+ is then the predominant ion, but its low concentration requires special techniques to permit its study by spectroscopy.

The second difficulty is that although H_2^+ has a stable ground electronic state (D_0^0=2.6507 eV) its first excited state is entirely repulsive and does not, therefore, give rise to a discrete electronic spectrum. Two excited electronic states are predicted to be weakly bound, but they are more than 11 eV

[illegible] methods.

In section II we review the development of the theory, from the introduction of the Schrodinger equation through to the present. In section III we give a comprehensive description of the theory as it is understood at present, and we draw attention to areas which still deserve closer attention. In section IV we describe photoelectron, photoionisation and photodissociation studies and in section V review investigations of the radiofrequency spectra. Finally in section VI we describe recent studies of the vibration-rotation spectra of the HD^+ ion which have provided accurate data for the vibrational and rotational levels of the ground electronic state. The balance of the discussion in this review is tilted strongly in the direction of the theory; that is but a reflection of the present position with regard to this, the simplest of all molecules.

II. HISTORICAL SURVEY OF THE THEORY

A very large number of papers have been published on the theory of the H_2^+ ion, and in this review we can only give an outline of how the theory has developed. The emphasis will be on work leading to the prediction or explanation of properties which can be measured experimentally. A detailed mathematical treatment is deferred to the next section; our historical survey of the development of the theory will be essentially descriptive.

The hydrogen molecular ion was first detected in the laboratory by J.J.Thomson in 1907 [3]. Attempts were made to describe H_2^+, treated as two fixed protons and a moving electron, within the framework of the old quantum theory [4] (phase integral quantisation of classical motion). But by 1926 the deficiencies of the old quantum theory were apparent and Schrodinger

proposed the wave equation [5]. The equation was soon applied to the problem of two fixed protons and a moving electron. By using elliptical coordinates (R,η,ξ) the three-dimensional wave equation separates into three one-dimensional differential equations [6]. The problem can therefore be solved exactly by numerical integration methods, and the first successful solution was obtained by Burrau [7] in 1927 who calculated the electronic energy of the ion in its ground state as a function of internuclear distance. Also in 1927, Born and Oppenheimer [8] gave their now famous justification for treating the nuclei as fixed as a first approximation in molecular quantum mechanics. Approximate methods of obtaining the electronic energy for various states by perturbation theory were investigated by a number of authors [9-12], whilst others applied the variation method [13,14]. These papers were the first to treat the excited states of H_2^+. Using these results Condon [15] was able to predict the behaviour of hydrogen under electron impact ionisation by electrons with different energies. Subsequent experimental work in 1930 [16,17] confirmed the predictions, a major success for the quantum treatment of H_2^+.

Methods for solving the separated electronic equations exactly by series expansion techniques were investigated in some detail by Wilson in 1928 [18]. These methods were further explored and applied by Hylleraas [19] and by Jaffé [20]. Specifically the expansions used by Hylleraas were:

$$M(R;\eta) = \sum_{\ell=\lambda}^{\infty} f_\ell(R) P_\ell^\lambda(\eta)$$

$$L(R;\xi) = (\xi^2-1)^{\lambda/2} \exp(-x/2) \sum_{n=\lambda}^{\infty} \frac{g_n(R)}{n!} \mathcal{L}_n^\lambda(x)$$

$P_\ell^\lambda(\eta)$ is an associated Legendre function, $\mathcal{L}_n^\lambda(x)$ is an associated Laguerre function in $x=2p(\xi-1)$, and the definitions of the various parameters are given in section III. This expansion is suggested

by considering the exact atomic wavefunctions at the united atom limit (He^+).

The ξ expansion proposed by Jaffé was:

$$L(R;\xi) = (\xi^2-1)^{\lambda/2} (\xi+1)^\delta \exp(-p\xi) \sum_{n=0}^{\infty} g_n(R) [(\xi-1)/(\xi+1)]^n$$

The first three terms reduce the ξ equation to a form which can be solved by a rapidly convergent series in $(\xi-1)/(\xi+1)$. They also reproduce the united atom asymptotic behaviour at large ξ. An expansion in $(\xi-1)/(\xi+1)$ is convenient since the ξ range $+1 \leq \xi < \infty$ is mapped onto $0 \leq [(\xi-1)/(\xi+1)] < 1$.

Both authors proceeded to obtain numerical solutions for the energy of H_2^+ by truncating the ξ and η expansions. They obtained relations between the energy, the separation constant in the differential equations, and the internuclear separation. Hylleraas calculated the energy at a number of internuclear separations by this method. He located the minimum of the internuclear potential energy curve close to 2.0 Bohr radii, with an energy of -1.2053 Rydbergs (relative to $2H^+ + e^-$). In order to obtain the zero point energy relative to this limit he fitted his results to a Morse potential function [21], obtaining 16.18 eV. The zero point dissociation energy of H_2^+ (to $H^+ + H$) is then 2.64 eV, a value subsequently confirmed by experiment [22].

The results of Jaffé's calculations agreed with those obtained by Hylleraas. The properties of the series expansions were reviewed in 1935 by Baber and Hassé [23]. Further calculations on H_2^+ using Jaffé's method were performed in 1935 by Sandeman [24], who fitted the potential he obtained to a Dunham expansion [25]. A comparison between these theoretical results and the available experimental estimates, obtained by the analysis of Rydberg spectra of H_2, can be found in a review by Richardson [26].

By 1935 the mathematical problems involved in obtaining exact electronic energies for H_2^+ (within the Born-Oppenheimer approximation)

had been solved, but it was not until the development of fast computational methods that this work could be explored fully. Extensive tabulations of the results of numerical solutions to the problem appeared during the 1950's and early 1960's [27-30]. From the electronic wavefunctions which were obtained various other physical properties were calculated. Bates calculated the electronic transition moment between the ground state and first excited state as a function of the internuclear separation [31]. The nuclear hyperfine interactions were considered by Dalgarno, Patterson and Somerville [32] and also by Stephen and Auffray [33]. Vibration-rotation energy levels were calculated by Cohen, Hiskes and Riddell [34] and by Wind [35] for H_2^+, and by Dunn [36] for D_2^+.

During the 1960's the need to take the calculations beyond the Born-Oppenheimer (clamped nuclei) limit became apparent, especially after the important paper on a nonadiabatic theory for diatomic molecules published by Kolos and Wolniewicz in 1963 [37]. Many years earlier Van Vleck [38] had pointed out that corrections to the clamped nuclei calculations would be needed to obtain the highest accuracy in calculations on diatomic molecules. The diagonal (adiabatic) corrections to the energy due to nuclear motion were calculated at various internuclear separations for H_2^+ as early as 1941 [39]. The application of the Born-Oppenheimer separation to three-particle systems was investigated in detail by Hunter, Pritchard and Gray [40-42]. As part of this work they performed adiabatic, and subsequently the first large scale nonadiabatic calculations, on the hydrogen molecular ion. The calculations were carried out by evaluating the nonadiabatic coupling between the ground state and the first few excited states of H_2^+, HD^+ and D_2^+; exact (within the Born-Oppenheimer limit) electronic wavefunctions were used for all states considered.

Much of the recent [illegible]

ion has been devoted to obtaining increasingly accurate vibration-rotation energy levels. Reviews of such work have been given by Kolos [43], and more recently by Bishop and Cheung [44]. This work has become increasingly important in view of recent measurements of high resolution infrared spectra of HD^+ [45,46], which are described in detail in a later section of this review. During the early 1970's calculations to the adiabatic limit (inclusion of the diagonal corrections to the internuclear potential due to nuclear motion) of the vibration-rotation levels of H_2^+ and its isotopic modifications have been performed by various authors [47-52]. The paper by Hunter, Yau and Pritchard [49] gives a complete tabulation of the vibration-rotation energy levels for HD^+, HT^+ and DT^+. Bishop [51] gives a similar tabulation, whilst Bishop and Wetmore [50] have listed the adiabatic corrections as a function of the internuclear separation. Adiabatic calculations have also been performed for two of the excited states of H_2^+ [53].

More recently nonadiabatic calculations have been performed. Estimates of the size and effects of nonadiabatic coupling on the ground state vibration-rotation levels can be made by perturbation theory [50]. Performing complete and accurate nonadiabatic calculations is, however, a daunting task since the electronic and nuclear motions cannot be treated separately. Two methods have been used to perform accurate nonadiabatic calculations. In the first, due to Kolos [47] and pursued by Bishop [54,55], a variational solution to the complete non-relativistic Hamiltonian of the three-particle system is sought. By using a very large expansion over products of functions to describe the electronic and nuclear motions (up to 515 functions were used) energies were obtained for the first few non-rotating vibrational states of H_2^+, D_2^+, HD^+, HT^+ and DT^+ with an estimated accuracy of ± 0.002 cm^{-1}. The [illegible]

of an approximate formula [56].

Wolniewicz and Poll [57,58] have devised a different method for performing nonadiabatic calculations which appears to be more elegant and efficient. They treated the nonadiabatic coupling between the ground and excited states as a perturbation to the adiabatic solution. The first-order perturbation to the adiabatic wavefunction was obtained variationally using expansions of the same form as the exact wavefunctions for the excited states which can couple directly to the ground state. Using this modified wavefunction they then obtained the nonadiabatic correction to the adiabatic vibration-rotation energy as the second-order energy correction. They tabulated the nonadiabatic energies obtained for HD^+ with v=0 to 21 and N=0 to 5, with an anticipated accuracy of 0.001 cm^{-1} [58]. These calculations represent the present state of the art, and are probably the most accurate calculations yet carried out for any molecule.

Other methods have been proposed for performing nonadiabatic calculations; for example, the generator coordinate method has received some attention [59], although numerical results have yet to be obtained.

In obtaining the most accurate vibration-rotation energies possible there are a number of other small effects to be considered, particularly relativistic and radiative corrections. The relativistic corrections allow for the fact that the Schrodinger equation is used rather than the Dirac equation. These corrections have been investigated in 1969 by Luke et al [60] and more recently by Gonsalves and Moss [61]; accurate calculations of the corrections were made by Bishop in 1977 [62]. The radiative corrections arise from the interaction of the electron with the zero point electromagnetic field. The Lamb shift due to this interaction

was first calculated for H_2^+ by Gersten [63], whilst Bishop and Cheung have performed further calculations for H_2^+ [64], and more recently for HD^+ [65]. Both the relativistic and radiative corrections were included in the nonadiabatic calculations of Bishop and Cheung [55] and of Wolniewicz and Poll [58].

Other work during the 1970's was concerned with the evaluation of properties of the hydrogen molecular ion which can be investigated experimentally. These calculations have generally used the exact Born-Oppenheimer electronic wavefunctions and adiabatic nuclear wavefunctions [50]. Examples include the study of hyperfine interactions by McEachran, Veenstra and Cohen [66] for H_2^+, and by Ray and Certain [67] for H_2^+ and HD^+. Both groups obtained excellent agreement with the available experimental data [68,45] which will be discussed in detail later. The photodissociation of H_2^+ and its isotopic modifications has also received considerable attention, starting with the work of Dunn in 1968 [69,70]. More recently Tadjeddine and Parlant [71] studied HD^+, and their results may be compared with the experimental work of van Asselt, Maas and Los [72] described in section IV. Photodissociation by infrared lasers has been considered theoretically by Fournier et al [73] and observed in the experiments described by Carrington and Buttenshaw [46]. Transition dipole moments for a number of infrared transitions of HD^+, HT^+ and DT^+ have been estimated [74,56]. Matrix elements of a number of other operators, averaged over vibrational state, have been given by Bishop and Cheung [75]. Rotationally-quasibound levels have been considered by Peek, Maas and Los [76], and Peek [77] has also drawn attention to the importance of long-range forces in H_2^+ and their effects on the potential curve for the first excited electronic state.

Despite the large amount of theoretical work on the hydrogen molecular ion which has been described, important problems still

[illegible] frequencies measured for HD^+ [45] [illegible] with the theory of Wolniewicz and Poll [58] to the expected level of accuracy, so that further refinement of the calculations is required. Hyperfine constants for the high vibrational levels of HD^+ studied by Carrington and Buttenshaw [46] have not yet been calculated even within the adiabatic approximation. Improvements in the range and quality of experimental measurements are likely, and could lead to improved values of certain fundamental constants provided the molecular quantum mechanics is sufficiently accurate.

III. PRESENT STATE OF THE THEORY

In the previous section we reviewed the historical development of the theory of the hydrogen molecular ion. In this section we will give a mathematical treatment of the theory, leading up to the present best calculations, those of Wolniewicz and Poll [58] on HD^+. Although most of this material can be found elsewhere [37,41,43,47,50,54,57,58] we feel that a complete summary of the theory in one place is now required, and we hope that this section will satisfy this need.

(i) The complete non-relativistic Hamiltonian.

For a system of point charges interacting electrostatically and moving through field-free space the complete non-relativistic Hamiltonian can be written in the form

$$\mathcal{H} = \sum_i \frac{-\hbar^2 \nabla_i^2}{2m_i} + \sum_i \sum_{j\neq i} \frac{z_i z_j e^2}{4\pi\varepsilon_0 r_{ij}} \qquad (1)$$

where all the symbols have their usual meanings. In order to obtain a convenient form of this Hamiltonian for the hydrogen molecular ion, we separate out the motion of the centre of mass of all particles by applying the transformation

$$\begin{pmatrix} \underset{\sim}{r}_g \\ \underset{\sim}{R} \\ \underset{\sim}{R}_{cm} \end{pmatrix} = \begin{pmatrix} -\frac{1}{2} & -\frac{1}{2} & 1 \\ -1 & 1 & 0 \\ m_1/M & m_2/M & m_e/M \end{pmatrix} \begin{pmatrix} \underset{\sim}{r}_1 \\ \underset{\sim}{r}_2 \\ \underset{\sim}{r}_e \end{pmatrix} \qquad (2)$$

where $M=m_1+m_2+m_e$. The coordinate systems are illustrated in figure 1. $\underset{\sim}{r}_1$, $\underset{\sim}{r}_2$ and $\underset{\sim}{r}_e$ are the position vectors of the three particles relative to an arbitrary space-fixed origin. The new basis vectors are the internuclear vector $\underset{\sim}{R}$ ($=\underset{\sim}{r}_2-\underset{\sim}{r}_1$), the position of the centre of mass of the system relative to the space-fixed origin $\underset{\sim}{R}_{cm}$, and the position of the electron relative to the geometric centre of the nuclei $\underset{\sim}{r}_g$. The separation can be achieved by other transformations [40], but that described here is the one most commonly applied to the hydrogen molecular ion. Applying the transformation (2) to the kinetic energy operators in the Hamiltonian (1) we obtain

$$-\hbar^2 \sum_i \frac{\nabla_i^2}{2m_i} = -\hbar^2 \left(\frac{\nabla_g^2}{2m_e} + \frac{\nabla_R^2}{2\mu} + \frac{\nabla_g^2}{8\mu} + \frac{\nabla_g \cdot \nabla_R}{2\mu_a} + \frac{\nabla_{cm}^2}{2M} \right) \qquad (3)$$

where $1/\mu = (1/m_1)+(1/m_2)$ and $1/\mu_a = (1/m_1)-(1/m_2)$. Note that $1/\mu_a = 0$ for the homonuclear case, $m_1=m_2$. The electrostatic potential, V, is unchanged by the transformation:

$$V = \frac{e^2}{4\pi\varepsilon_0} \left(\frac{1}{R} - \frac{1}{r_{1e}} - \frac{1}{r_{2e}} \right) \qquad (4)$$

because it depends on the relative positions of the particles. The translational motion can now be separated out of the Schrodinger equation (5),

$$\left\{ -\hbar^2 \left[\frac{\nabla_g^2}{2m_e} + \frac{\nabla_R^2}{2\mu} + \frac{\nabla_g^2}{8\mu} + \frac{\nabla_g \cdot \nabla_R}{2\mu_a} + \frac{\nabla_{cm}^2}{2M} \right] + V \right\} \Psi_{tot} = E_{tot} \Psi_{tot} \qquad (5)$$

We use the form $\Psi_{tot}(\underset{\sim}{R}_{cm}, \underset{\sim}{R}, \underset{\sim}{r}_g) = A_{cm}(\underset{\sim}{R}_{cm}) \psi_{mol}(\underset{\sim}{R}, \underset{\sim}{r}_g)$ in order to achieve the separation, which is

$$\left\{ -\hbar^2 \left[\frac{\nabla_g^2}{2m_e} + \frac{\nabla_R^2}{2\mu} + \frac{\nabla_g^2}{8\mu} + \frac{\nabla_g \cdot \nabla_R}{2\mu_a} \right] + V \right\} \psi_{mol} = E_{int} \psi_{mol} \qquad (6)$$

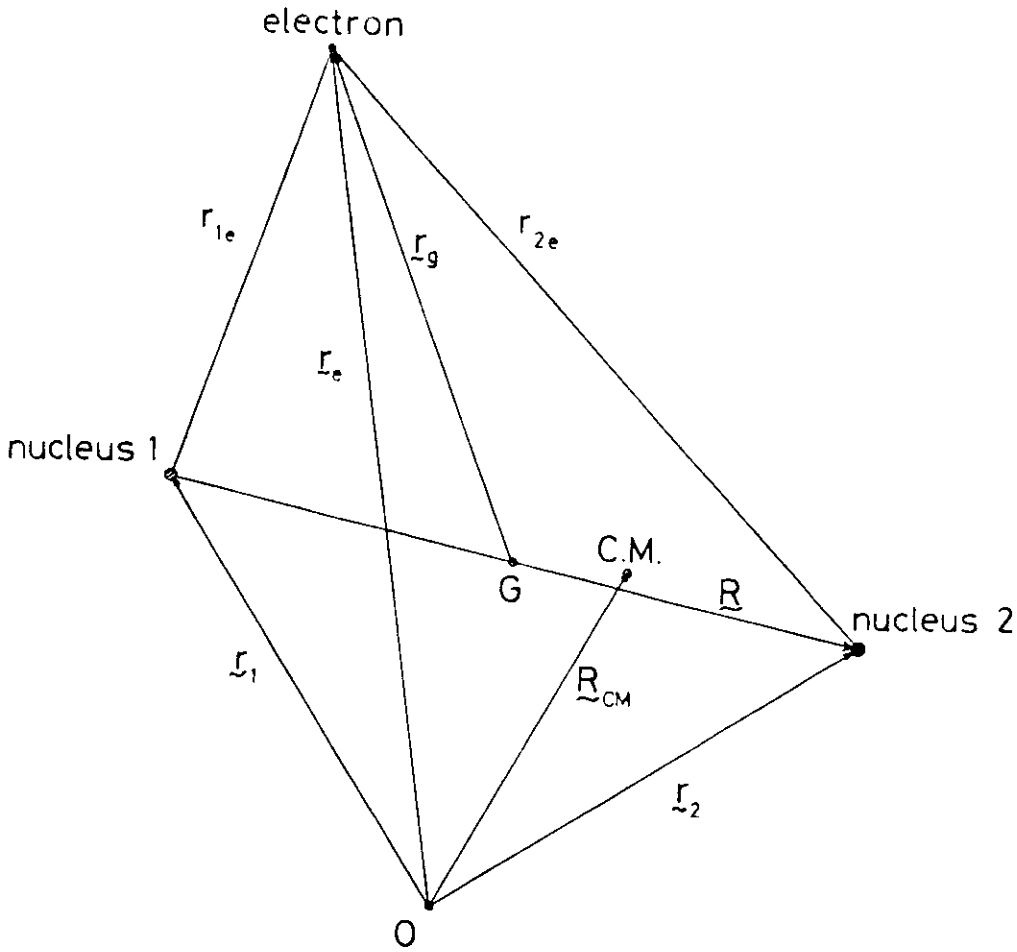

Figure 1

$$-\frac{\hbar^2}{2M}\nabla^2_{cm}\,A_{cm} = (E_{tot}-E_{int})A_{cm} \qquad (7)$$

Equation (7) is simply the time-independent Schrodinger equation for a body of mass M freely translating through space with kinetic energy $(E_{tot}-E_{int})$.

In summary, the non-relativistic Hamiltonian, in atomic units, for the internal motion of the hydrogen molecular ion is

$$\mathcal{H}_{int} = -\frac{\nabla^2_g}{2} - \frac{\nabla^2_R}{2\mu} - \frac{\nabla^2_g}{8\mu} - \frac{\nabla_g\cdot\nabla_R}{2\mu_a} + \frac{1}{R} - \frac{1}{r_{1e}} - \frac{1}{r_{2e}} \qquad (8)$$

(ii) Solution of the Schrodinger equation.

The non-relativistic Hamiltonian (8) contains terms which couple the electronic and nuclear motions; this makes it impossible to obtain exact eigenfunctions and eigenvalues. However by making certain approximations it it possible to reduce the problem to one which can be solved exactly. In order to see how this may be achieved we follow the method suggested by Born [78], and expand the complete molecular wavefunction as the series

$$\psi_{mol}(\underset{\sim}{R},\underset{\sim}{r}_g) = \sum_t F_t(\underset{\sim}{R})\phi_t(R,\underset{\sim}{r}_g) \qquad (9)$$

where the $\phi_t(R,\underset{\sim}{r}_g)$ are the exact solutions of what we will call the electronic Born-Oppenheimer equation for the hydrogen molecular ion:

$$\left(-\frac{\nabla^2_g}{2} - \frac{1}{r_{1e}} - \frac{1}{r_{2e}} + \frac{1}{R}\right)\phi_t(R,\underset{\sim}{r}_g) = E_t(R)\phi_t(R,\underset{\sim}{r}_g) \qquad (10)$$

The methods for solving this equation are well established [41] and we will describe them later. Substituting the Born expansion (9) into the complete non-relativistic Schrodinger equation (8) we obtain a set of coupled differential equations for the functions $F_t(\underset{\sim}{R})$:

$$\mathcal{H}_{int}\sum_t F_t(\underset{\sim}{R})\phi_t(R,\underset{\sim}{r}_g) = E_{int}\sum_t F_t(\underset{\sim}{R})\phi_t(R,\underset{\sim}{r}_g) \qquad (11)$$

The equation is simplified by premultiplying by $\phi^*_s(R,\underset{\sim}{r}_g)$ and

integrating over the electronic coordinates r_g to obtain

$$E_s(R)F_s(\underset{\sim}{R}) + \int\phi_s^*(R,\underset{\sim}{r}_g)\left[-\frac{\nabla_R^2}{2\mu} - \frac{\nabla_g^2}{8\mu} - \frac{\underset{\sim}{\nabla}_g\cdot\underset{\sim}{\nabla}_R}{2\mu_a}\right]F_s(\underset{\sim}{R})\phi_s(R,\underset{\sim}{r}_g)d\underset{\sim}{r}_g$$

$$+ \sum_{t\neq s}\int\phi_s^*(R,\underset{\sim}{r}_g)\left[-\frac{\nabla_R^2}{2\mu} - \frac{\nabla_g^2}{8\mu} - \frac{\underset{\sim}{\nabla}_g\cdot\underset{\sim}{\nabla}_R}{2\mu_a}\right]F_t(\underset{\sim}{R})\phi_t(R,\underset{\sim}{r}_g)d\underset{\sim}{r}_g = E_{int}F_s(\underset{\sim}{R}) \qquad (12)$$

Since in the electronic Born-Oppenheimer equation (10) the nuclei are implicitly treated as fixed point charges, the functions $\phi_t(R,\underset{\sim}{r}_g)$ must be either symmetric or antisymmetric with respect to exchange of nuclei and electron inversion through the geometric centre of the nuclei. The operator $\underset{\sim}{\nabla}_R$ is antisymmetric with respect to nuclear permutation, whilst $\underset{\sim}{\nabla}_g$ is antisymmetric under electron inversion. Consequently by symmetry we have

$$\int\phi_s^*(R,\underset{\sim}{r}_g)\underset{\sim}{\nabla}_R\,\phi_s(R,\underset{\sim}{r}_g)\,d\underset{\sim}{r}_g = 0$$

$$\int\phi_s^*(R,\underset{\sim}{r}_g)\underset{\sim}{\nabla}_g\,\phi_s(R,\underset{\sim}{r}_g)\,d\underset{\sim}{r}_g = 0$$

$$\int\phi_s^*(R,\underset{\sim}{r}_g)\underset{\sim}{\nabla}_g\cdot\underset{\sim}{\nabla}_R\,\phi_s(R,\underset{\sim}{r}_g)\,d\underset{\sim}{r}_g = 0 \qquad (13)$$

so that equation (12) becomes:

$$\left[E_s(R) - \frac{\nabla_R^2}{2\mu} - \int\phi_s^*(R,\underset{\sim}{r}_g)\left[\frac{\nabla_g^2}{8\mu} + \frac{\nabla_R^2}{2\mu}\right]\phi_s(R,\underset{\sim}{r}_g)d\underset{\sim}{r}_g\right]F_s(\underset{\sim}{R})$$

$$+ \sum_{t\neq s}\left\{\int\phi_s^*(R,\underset{\sim}{r}_g)\left[-\frac{\nabla_R^2}{2\mu} - \frac{\nabla_g^2}{8\mu} - \frac{\underset{\sim}{\nabla}_g\cdot\underset{\sim}{\nabla}_R}{2\mu_a}\right]\phi_t(R,\underset{\sim}{r}_g)d\underset{\sim}{r}_g\right.$$

$$\left. + \int\phi_s^*(R,\underset{\sim}{r}_g)\left[-\frac{\underset{\sim}{\nabla}_R}{2\mu} - \frac{\underset{\sim}{\nabla}_g}{2\mu_a}\right]\phi_t(R,\underset{\sim}{r}_g)d\underset{\sim}{r}_g\cdot\underset{\sim}{\nabla}_R\right\}F_t(\underset{\sim}{R}) = E_{int}F_s(\underset{\sim}{R}) \qquad (14)$$

An exact solution of this set of coupled differential equations is not feasible since the couplings between the infinite set of functions $F_t(\underset{\sim}{R})\phi_t(R,\underset{\sim}{r}_g)$ would have to be considered. In practice it is necessary to neglect some of the couplings in order to make the problem tractable, or to seek an alternative method of solving the problem.

(iii) The electronic Born-Oppenheimer equation.

Before proceeding to describe the approximations that can be made to simplify equation (14) we return to the electronic Born-Oppenheimer equation (10). Historically this equation was the starting point of the modern quantum theory of the hydrogen molecular ion [19,20]. The problem is to solve for the motion of a single electron about two fixed nuclear charge centres. By using prolate spheroidal coordinates the three-dimensional equation (10) separates into three one-dimensional equations. Figure 2 shows the cartesian coordinate system; the prolate spheroidal coordinates are:

$$\xi = \frac{(r_{1e}+r_{2e})}{R} \text{ with } 1\leq\xi<\infty \;;\quad \eta = \frac{(r_{1e}-r_{2e})}{R} \text{ with } -1\leq\eta\leq 1 \qquad (15)$$

and χ, rotation of the electron about the z axis ($0\leq\chi<2\pi$). In this coordinate system we have

$$\underset{\sim}{\nabla}_g = \frac{\partial}{\partial x}\underset{\sim}{i} + \frac{\partial}{\partial y}\underset{\sim}{j} + \frac{\partial}{\partial z}\underset{\sim}{k}$$

$$= \frac{2[(\xi^2-1)(1-\eta^2)]^{\frac{1}{2}}}{R(\xi^2-\eta^2)}\left\{\left[\xi\cos\chi\frac{\partial}{\partial\xi} - \eta\cos\chi\frac{\partial}{\partial\eta} - \frac{\sin\chi(\xi^2-\eta^2)}{(\xi^2-1)(1-\eta^2)}\right]\underset{\sim}{i}\right.$$

$$+ \left[\xi\sin\chi\frac{\partial}{\partial\xi} - \eta\sin\chi\frac{\partial}{\partial\eta} + \frac{\cos\chi(\xi^2-\eta^2)}{(\xi^2-1)(1-\eta^2)}\right]\underset{\sim}{j}$$

$$\left. + \left[\frac{\eta(\xi^2-1)^{\frac{1}{2}}}{(1-\eta^2)^{\frac{1}{2}}}\frac{\partial}{\partial\xi} + \frac{\xi(1-\eta^2)^{\frac{1}{2}}}{(\xi^2-1)^{\frac{1}{2}}}\frac{\partial}{\partial\eta}\right]\underset{\sim}{k}\right\} \qquad (16)$$

The Laplacian operator in the new coordinates is

$$\nabla_g^2 = \frac{4}{R^2(\xi^2-\eta^2)}\left\{\frac{\partial}{\partial\xi}(\xi^2-1)\frac{\partial}{\partial\xi} + \frac{\partial}{\partial\eta}(1-\eta^2)\frac{\partial}{\partial\eta} + \frac{(\xi^2-\eta^2)}{(\xi^2-1)(1-\eta^2)}\frac{\partial^2}{\partial\chi^2}\right\} \qquad (17)$$

and the volume element is

$$d\underset{\sim}{r}_g = \frac{R^3(\xi^2-\eta^2)}{8}\,d\xi\,d\eta\,d\chi \qquad (18)$$

The electron-nuclear electrostatic attraction operator may also be transformed into the (ξ,η,χ) coordinate system, with the result

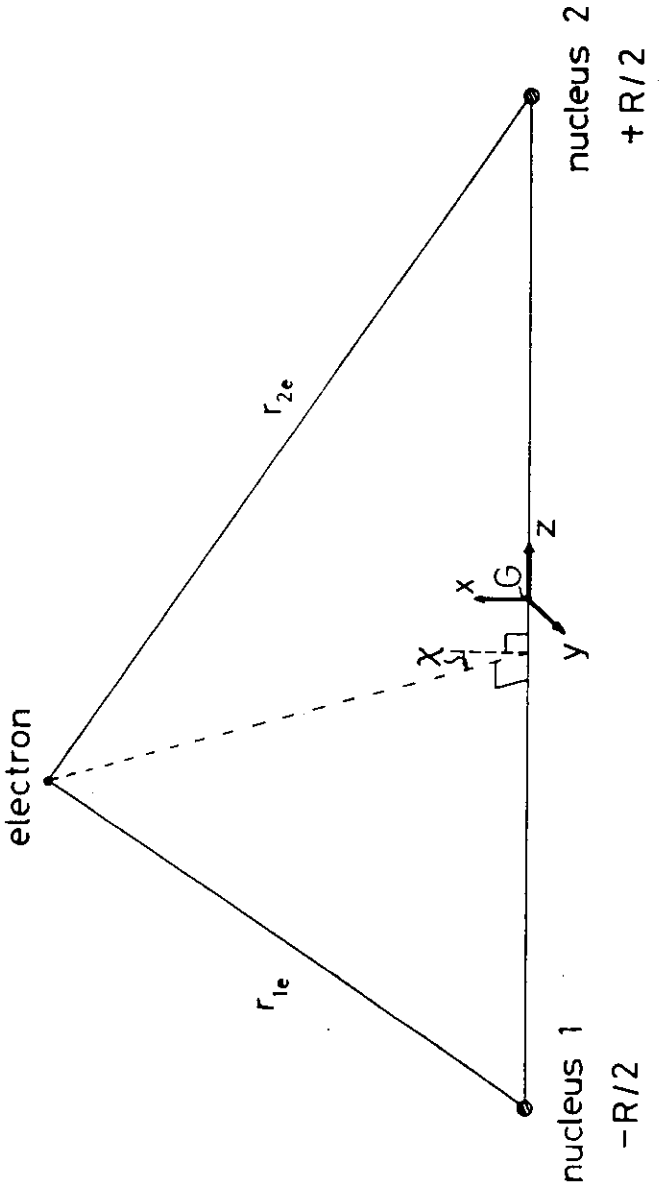

Figure 2

$$-1/r_{1e} - 1/r_{2e} = -4\xi/R(\xi^2-\eta^2) \qquad (19)$$

Consequently in prolate spheroidal coordinates the electronic Born-Oppenheimer equation becomes

$$\left[-\frac{2}{R^2(\xi^2-\eta^2)}\left\{\frac{\partial}{\partial\xi}(\xi^2-1)\frac{\partial}{\partial\xi}+\frac{\partial}{\partial\eta}(1-\eta^2)\frac{\partial}{\partial\eta}+\frac{(\xi^2-\eta^2)}{(\xi^2-1)(1-\eta^2)}\frac{\partial^2}{\partial\chi^2}\right\}\right.$$
$$\left.-\frac{4\xi}{R(\xi^2-\eta^2)}+\frac{1}{R}\right]\phi_t(R,\xi,\eta,\chi) = E_t(R)\phi_t(R,\xi,\eta,\chi) \qquad (20)$$

which may be written in the more compact form

$$\left[\frac{\partial}{\partial\xi}(\xi^2-1)\frac{\partial}{\partial\xi}+\frac{\partial}{\partial\eta}(1-\eta^2)\frac{\partial}{\partial\eta}+\left\{\frac{1}{(\xi^2-1)}+\frac{1}{(1-\eta^2)}\right\}\frac{\partial^2}{\partial\chi^2}+2R\xi-p^2(\xi^2-\eta^2)\right]\phi_t(R,\xi,\eta,\chi)$$
$$= 0 \qquad (21)$$

where $p^2 = -[E_t(R)-(1/R)]R^2/2.$

The separation into three one-dimensional equations is now easily achieved by making the substitution

$$\phi_t(R,\xi,\eta,\chi) = L(R,\xi)M(R,\eta)N(\chi) \qquad (22)$$

We then obtain the three separated equations:

$$\left[\frac{\partial^2}{\partial\chi^2}+\Lambda^2\right]N = 0$$
$$\left[\frac{\partial}{\partial\xi}(\xi^2-1)\frac{\partial}{\partial\xi}+A-\frac{\Lambda^2}{(\xi^2-1)}+2R\xi-p^2\xi^2\right]L = 0$$
$$\left[\frac{\partial}{\partial\eta}(1-\eta^2)\frac{\partial}{\partial\eta}-A-\frac{\Lambda^2}{(1-\eta^2)}+p^2\eta^2\right]M = 0 \qquad (23)$$

where Λ^2 and A are the separation constants.

The χ equation can be solved analytically, with the result

$$N(\chi) = \frac{\exp(i\Lambda\chi)}{(2\pi)^{\frac{1}{2}}} \qquad \text{where } \Lambda=0,\pm1,\pm2,\ldots \qquad (24)$$

Certain aspects of the symmetry of the problem are evident from equations (23). Λ appears as Λ^2 in the ξ and η equations, so that the eigenvalues have a twofold degeneracy for $\Lambda\neq0$, due to the cylindrical symmetry of the system. The η equation is invariant to the operation $\eta\rightarrow-\eta$, so that the equation possesses separate even and odd solutions for each value of A, caused by the nuclear permutation symmetry of the system.

In order to obtain a numerical solution of the ξ equation we will consider the Jaffé expansion

$$L(R,\xi) = (\xi^2-1)^{\Lambda/2}(\xi+1)^{\delta'} \exp(-p\xi) \sum_{n=0}^{\infty} g_n(R)[(\xi-1)/(\xi+1)]^n \qquad (25)$$

where $\delta'=(R/p)-\Lambda-1$. Substitution of this expansion into (23) leads to a recursion relation between the coefficients $g_n(R)$,

$$g_{n+1}[(n+1)(n+\Lambda+1)] + g_n[A-p^2+2p\delta+(\delta'+\Lambda)(\Lambda+1)+2n(\delta'-2p)-2n^2] + g_{n-1}[(n-\delta'-1)(n-\delta'-\Lambda-1)] = 0 \qquad (26)$$

We further require $g_n=0$ for $n<0$, and for numerical calculations we truncate the series so that $g_n=0$ for $n>n_{max}$ (the series converges rapidly). The set of recursion relations (26) may then be written as a matrix eigenvalue equation [41],

$$\underset{\sim}{G}\cdot\underset{\sim}{g} = -A\underset{\sim}{g} \qquad (27)$$

where

$$\underset{\sim}{g} = \begin{pmatrix} g_0 \\ g_1 \\ \cdot \\ \cdot \\ g_{n_{max}} \end{pmatrix}$$

and the non-zero elements of the tridiagonal matrix $\underset{\sim}{G}$ are

$$\begin{aligned} G_{n-1,n} &= (n-\delta-1)(n-\delta'-\Lambda-1) \\ G_{n,n} &= -p^2+2p\delta'+(\delta'+\Lambda)(\Lambda+1)+2n(\delta'-2p)-2n^2 \\ G_{n+1,n} &= (n+1)(n+\Lambda+1) \end{aligned} \qquad (28)$$

Other expansions, notably that due to Hylleraas [19], have been used to solve the ξ equation; they also lead to recursion relations which may be expressed as matrix eigenvalue equations.

The η equation may be solved by using an expansion over associated Legendre functions,

$$M(R,\eta) = \sum_{s=0}^{\infty} f_s(R) P_{\Lambda+s}^{\Lambda}(\eta) \qquad (29)$$

Because of the symmetry of the η equation only odd or even terms will appear in the expansion for a given state. Substituting the expansion (29) into (23) and using the known properties of the functions $P_{\Lambda+s}^{\Lambda}(\eta)$:

$$\left[\frac{d}{d\eta}(1-\eta^2)\frac{d}{d\eta} - \frac{\Lambda^2}{(1-\eta^2)} + (\Lambda+s)(\Lambda+s+1)\right] P_{\Lambda+s}^{\Lambda}(\eta) = 0$$

$$(s+1)P_{\Lambda+s+1}^{\Lambda}(\eta) - (2\Lambda+2s+1)\eta P_{\Lambda+s}^{\Lambda}(\eta) + (2\Lambda+s)P_{\Lambda+s-1}^{\Lambda}(\eta) = 0 \qquad (30)$$

we obtain a recursion relation between the coefficients $f_s(R)$,

$$f_{s-2}\left[\frac{-p^2(s-1)s}{(2\Lambda+2s-3)(2\Lambda+2s-1)}\right] + f_s\left[(\Lambda+s)(\Lambda+s+1) - \frac{p^2(2\Lambda+s)s}{(2\Lambda+2s-1)(2\Lambda+2s+1)} - \frac{p^2(2\Lambda+s+1)(s+1)}{(2\Lambda+2s+1)(2\Lambda+2s+3)} + A\right] + f_{s+2}\left[\frac{-p^2(2\Lambda+s+1)(2\Lambda+s+2)}{(2\Lambda+2s+3)(2\Lambda+2s+5)}\right] = 0 \qquad (31)$$

As in the case of the ξ equation this set of recursion relations may be expressed as a matrix eigenvalue equation [41],

$$\underset{\sim}{F}\cdot\underset{\sim}{f} = A\underset{\sim}{f} \qquad (32)$$

where

$$\underset{\sim}{f} = \begin{pmatrix} f_0 \\ f_2 \\ \cdot \\ \cdot \\ f_{2N} \end{pmatrix} \quad \text{or} \quad \underset{\sim}{f} = \begin{pmatrix} f_1 \\ f_3 \\ \cdot \\ \cdot \\ f_{2N+1} \end{pmatrix}$$

for even (g symmetry) or odd (u symmetry) states respectively. The non-zero elements of the matrix $\underset{\sim}{F}$ are then given by

$$\begin{aligned} F_{s-2,s} &= \frac{p^2(s-1)s}{(2\Lambda+2s-3)(2\Lambda+2s-1)} \\ F_{s,s} &= -(\Lambda+s)(\Lambda+s+1) + \frac{p^2}{(2\Lambda+2s+1)}\left\{\frac{(2\Lambda+s)s}{(2\Lambda+2s-1)} + \frac{(2\Lambda+s+1)(s+1)}{(2\Lambda+2s+3)}\right\} \\ F_{s+2,s} &= \frac{p^2(2\Lambda+s+1)(2\Lambda+s+2)}{(2\Lambda+2s+3)(2\Lambda+2s+5)} \end{aligned} \qquad (33)$$

The solution of the electronic Born-Oppenheimer equation (10), determining $f(R)$, $g(R)$ and $E_t(R)$ for a given state at a particular R value, is achieved by requiring that A simultaneously satisfies equations (27) and (32). Numerical methods have been outlined by Hunter and Pritchard [41]; the problem is particularly simple for the hydrogen molecular ion because both $\underset{\sim}{F}$ and $\underset{\sim}{G}$ are tridiagonal matrices. The results of such calculations can be found in many places; see, for example, the paper by Peek [30].

(iv) Levels of approximation.

(a) The Born-Oppenheimer approximation.

At this level of approximation all terms coupling the electronic and nuclear motions are neglected. Equation (14) then reduces to the Born-Oppenheimer equation for nuclear motion:

$$\left\{E_s(R) - \frac{\nabla_R^2}{2\mu}\right\} F_s^{BO}(\underset{\sim}{R}) = E_{int}^{BO} F_s^{BO}(\underset{\sim}{R}) \qquad (34)$$

The advantage of this approximation is the great simplification we achieve over equation (14). However this simplification is achieved at the expense of a considerable loss of accuracy in any calculations.

(b) The adiabatic approximation.

The adiabatic approximation has been extensively reviewed by Kolos [43]. At this level of approximation we retain the terms coupling the electronic and nuclear motions which are diagonal in the electronic state; equation (14) reduces to

$$\left\{E_s(R) - \int \phi_s^*(R,\underset{\sim}{r}_g)\frac{\nabla_g^2}{8\mu}\phi_s(R,\underset{\sim}{r}_g)d\underset{\sim}{r}_g - \int \phi_s^*(R,\underset{\sim}{r}_g)\frac{\nabla_R^2}{2\mu}\phi_s(R,\underset{\sim}{r}_g)d\underset{\sim}{r}_g - \frac{\nabla_R^2}{2\mu}\right\} F_s^{AD}(\underset{\sim}{R})$$
$$= E_{int}^{AD} F_s^{AD}(\underset{\sim}{R}) \qquad (35)$$

The effect of the approximation is that the nuclear motion is now governed by an effective potential

$$E_s(R) - \int \phi_s^*(R,\underset{\sim}{r}_g)\frac{\nabla_g^2}{8\mu}\phi_s(R,\underset{\sim}{r}_g)d\underset{\sim}{r}_g - \int \phi_s^*(R,\underset{\sim}{r}_g)\frac{\nabla_R^2}{2\mu}\phi_s(R,\underset{\sim}{r}_g)d\underset{\sim}{r}_g \qquad (36)$$

obtained by averaging the complete Hamiltonian (8) over the Born-Oppenheimer electronic wavefunction $\phi_s(R,\underset{\sim}{r}_g)$. The effective adiabatic potential (36) is isotope dependent, because of its dependence on μ. The Born-Oppenheimer potential $E_s(R)$ is isotope independent. Working at this level of approximation we retain the basic simplicity of the Born-Oppenheimer equation for nuclear motion, equation (34), because the electronic and nuclear motions are effectively separated. But because we have included the diagonal corrections, calculations made within the adiabatic

approximation will be more accurate. The adiabatic approximation is particularly successful when there are no close-lying states which are non-adiabatically coupled to the state of interest. This is the case for the ground electronic state of H_2^+ and D_2^+, but for the heteronuclear system HD^+ the $\nabla_g.\nabla_R/2\mu_a$ term in equation (14) ($1/\mu_a=0$ for homonuclear systems) couples the ground (Σ_g) and first excited (Σ_u) electronic states. In order to obtain accurate results for HD^+ it will be necessary to perform nonadiabatic calculations, particularly for the high vibrational levels. The problem can be illustrated by considering the behaviour of the adiabatic potentials for these states at large R. Within the adiabatic treatment they are identical at very large R, yet in reality the dissociation limits $H^+ + D(^1S)$ and $H(^1S) + D^+$ are separated by 29.8 cm^{-1}. This degeneracy is lifted by nonadiabatic coupling.

Hunter, Yau and Pritchard [49] have given an extensive tabulation of the results of adiabatic calculations of vibration-rotation levels of the ground electronic state of H_2^+, D_2^+ and HD^+. Bishop and Wetmore [50] have provided values for the adiabatic corrections to the potential, $-\int \phi_s^*(R,\underset{\sim}{r}_g)(\nabla_g^2/8\mu)\phi_s(R,\underset{\sim}{r}_g)d\underset{\sim}{r}_g$ and $-\int \phi_s^*(R,\underset{\sim}{r}_g)(\nabla_R^2/2\mu)\phi_s(R,\underset{\sim}{r}_g)d\underset{\sim}{r}_g$. Figure 3 is a plot of the Born-Oppenheimer potential $E_s(R)$, and the adiabatic corrections, which are both positive, for the ground electronic state of H_2^+.

The adiabatic approximation is widely used for calculating other properties of the hydrogen molecular ion, bacause of the convenient separation it allows of the electronic and nuclear motions through the use of an effective potential. Evaluation of properties for a given vibration-rotation state is achieved by averaging electronic matrix elements obtained from the $\phi_s(R,\underset{\sim}{r}_g)$ over the adiabatic vibration-rotation wavefunction $F_s^{AD}(\underset{\sim}{R})$. A good example is the calculation of nuclear hyperfine constants [67].

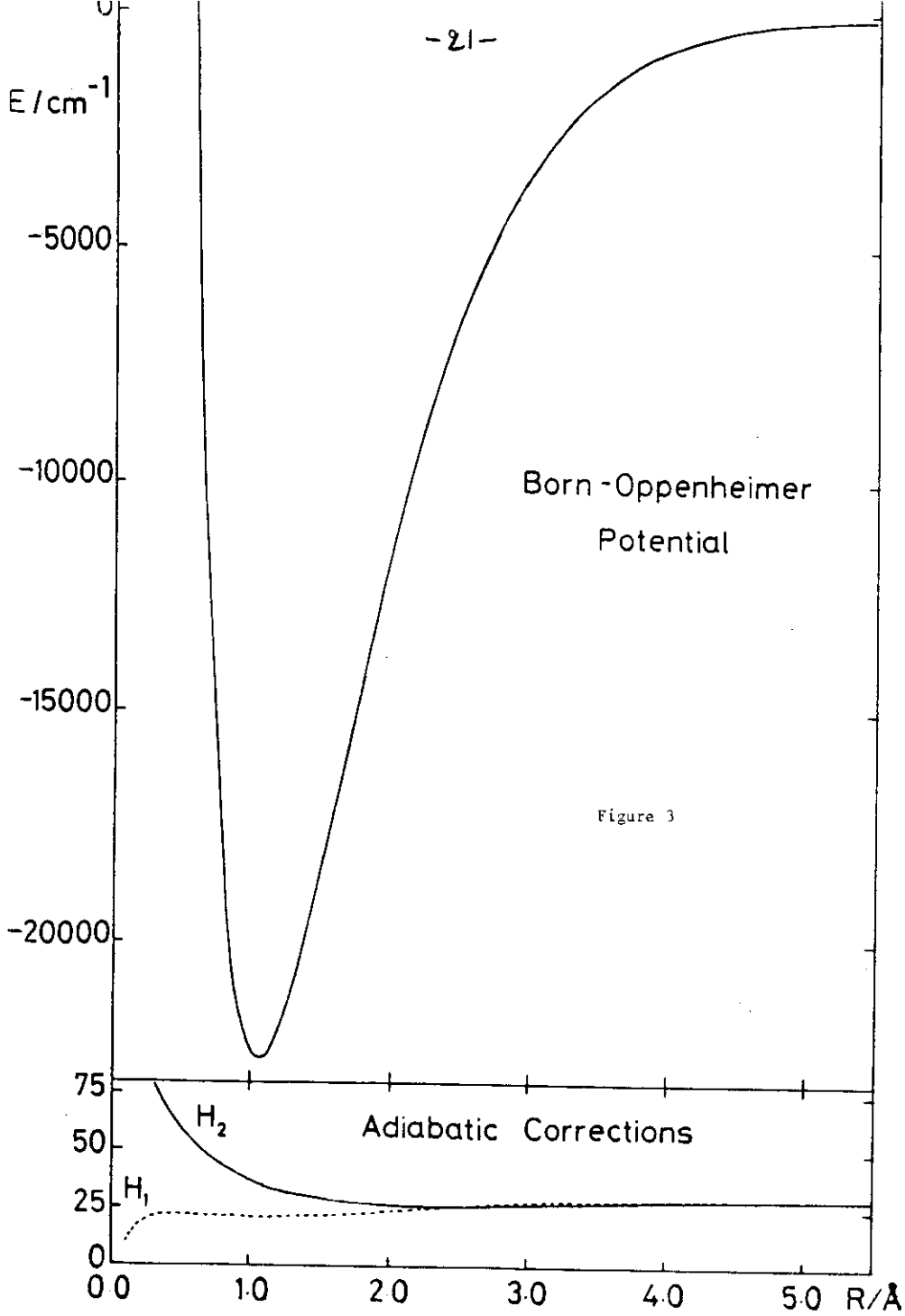

Figure 3

(c) Nonadiabatic calculations.

The exact solution of the nonadiabatic problem as expressed by (14) is impossible, as it requires the solution of an infinite set of coupled differential equations. Following the approximations described above we could reduce the problem by considering the coupling with only a limited number of other states, and hope that the Born expansion (9) converges rapidly. This approach was followed by Hunter and Pritchard [42] for the four lowest vibrational states of H_2^+, HD^+ and D_2^+, by investigating the convergence of the energy levels as progressively higher states $\phi_t(R,r_g)$ were included in the expansion (9). Initial rapid convergence was found for these low vibrational levels. In order to improve the accuracy of these calculations and extend them to higher vibrational levels, much longer Born expansions will be required. To perform efficient and accurate nonadiabatic calculations, alternative formulations of the problem are desirable, and two techniques have been investigated, which we now describe.

1. Variational approach.

In this method, investigated by Bishop [54] and by Bishop and Cheung [55], the eigenenergies of the complete Hamiltonian (8) are sought by variational adjustment of a trial wavefunction. Only a few low-lying non-rotating vibrational levels of the ground electronic state were considered, for various isotopic modifications of the hydrogen molecular ion. The trial wavefunction used was

$$\bar{\psi} = \sum_{i=0}^{i_m} \sum_{j=0,2}^{j_m} \sum_{k=0}^{k_m} C_{ijk}\phi_{ijk}(\xi,\eta,R) + \sum_{i=0}^{i_m'} \sum_{j=1,3}^{j_m} \sum_{k=0}^{k_m} C_{ijk}\phi_{ijk}(\xi,\eta,R) \qquad (37)$$

where the basis functions of the expansion were

$$\phi_{ijk}(\xi,\eta,R) = \exp(-\alpha\xi)\cosh(\beta\eta)\xi^i\eta^j R^{-3/2}\exp[\tfrac{1}{2}(-x^2)]H_k(x) \qquad (38)$$

The $H_k(x)$ are Hermite polynomials, $x=\gamma(R-\delta)$, and $\alpha, \beta, \gamma, \delta$ are adjustable parameters chosen to minimise the energy; with large expansions the values are not very critical. This basis was selected because the integrals required for a variational solution are easily evaluated [54]. Even and odd states are only mixed by the $\nabla_g \cdot \nabla_R / 2\mu_a$ term in the Hamiltonian, so that the second triple summation in the expansion only appears for heteronuclear systems like HD^+. The convergence of the variationally-calculated energies with respect to basis set size was investigated very carefully. The final results, obtained with an expansion of up to 515 terms, should be accurate to ± 0.001 cm^{-1}, after the inclusion of radiative and relativistic corrections [55]. Energies of the rotating states were also calculated by means of an approximate formula for the change in nonadiabatic energy correction with rotational quantum number [56]. Infrared transition frequencies accurate to ± 0.002 cm^{-1} could then be obtained for HD^+, and compared with the results of Wing et al [45].

2. Variation-Perturbation approach.

By using the variational approach, the problem of having to consider explicitly the couplings between the adiabatic states, described by (14), is avoided. However this method makes no use of the exact adiabatic eigenvalues and wavefunctions which can be readily obtained for the hydrogen molecular ion. As we have discussed, the adiabatic approximation is usually quite accurate, so that a method which makes use of the adiabatic solutions as a starting point for nonadiabatic calculations would appear to offer greater efficiency and elegance than the fully variational approach.

Wolniewicz and Poll [57,58] have developed such an alternative formulation of the problem, in which the nonadiabatic effects are treated as a perturbation to the adiabatic approximation. They define an adiabatic Hamiltonian $\mathcal{H}^{AD}$ by the equation

$$\mathcal{H}^{AD} = \sum_n E_n^{AD} |\psi_n^{AD}\rangle\langle\psi_n^{AD}| \tag{39}$$

such that its eigenvalues are the adiabatic molecular energy levels E_n^{AD}, and its eigenfunctions are the adiabatic states of the molecule,

$$\psi_n^{AD} = \phi_n^{BO}(R, \underset{\sim}{r}_g) F_n^{AD}(\underset{\sim}{R}) \tag{40}$$

which can be obtained exactly from (10) and (35). This abstract definition allows the complete non-relativistic Hamiltonian (8) to be decomposed into an adiabatic part, and a nonadiabatic term,

$$\mathcal{H} = \mathcal{H}^{AD} + \mathcal{H}'^{N.AD} \tag{41}$$

The methods of perturbation theory may now be used to calculate nonadiabatic corrections to the adiabatic energies E_n^{AD},

$$\mathcal{H}|\psi_n^{AD}\rangle = E_n^{AD}|\psi_n^{AD}\rangle + \mathcal{H}'^{N.AD}|\psi_n^{AD}\rangle \tag{42}$$

Since from (35) we have

$$\langle\psi_n^{AD}|\mathcal{H}|\psi_n^{AD}\rangle = E_n^{AD} \tag{43}$$

the first order nonadiabatic energy correction is zero:

$$\langle\psi_n^{AD}|\mathcal{H}'^{N.AD}|\psi_n^{AD}\rangle = 0 \tag{44}$$

The variation-perturbation method of Wolniewicz and Poll is to obtain the second order nonadiabatic energy corrections from the first order correction to the wavefunction,

$$\psi_n = \psi_n^{AD} + \psi_n' \tag{45}$$

The first order correction ψ_n' satisfies

$$(\mathcal{H}^{AD} - E_n^{AD})\psi_n' = -\mathcal{H}'^{N.AD}\psi_n^{AD} \tag{46}$$

where we have used (44). ψ_n' is obtained by solving this equation variationally. The nonadiabatic energy correction to second order in perturbation theory is then

$$E'' = \langle\psi_n'|\mathcal{H}'^{N.AD}|\psi^{AD}\rangle \tag{47}$$

Equation (46) from which the ψ_n' are to be obtained can be simplified by separating out those parts of the wavefunctions which describe their angular momentum:

$$\psi^{AD} = U^{AD}\Omega^J_{M\Lambda_0} \tag{48}$$

and

$$\psi' = \sum_\Lambda U_\Lambda \Omega^J_{M\Lambda} \tag{49}$$

where the $\Omega^J_{M\Lambda}$ are the eigenfunctions of a symmetric top, and the

[illegible] premultiplying by $\bar{\Lambda}^{*}_{M\Lambda}$ and integrating over the angular variables, (46) becomes

$$\left\{\langle JM\Lambda|\mathcal{H}^{AD}|JM\Lambda\rangle - E^{AD}\right\}U_{\Lambda} = -\langle JM\Lambda|\mathcal{H}'^{N.AD}|JM\Lambda_0\rangle\, U^{AD} \qquad (50)$$

Appropriate differential forms of the operators $\mathcal{H}^{AD}$ and $\mathcal{H}'^{N.AD}$ are obtained as follows. From equation (42) we have

$$\mathcal{H}'^{N.AD} = \mathcal{H} - E^{AD} \qquad (51)$$

whilst, as indicated in the Born development of the theory, the adiabatic Hamiltonian $\mathcal{H}^{AD}$, given by

$$\mathcal{H}^{AD} = -\frac{\nabla_R^2}{2} + \frac{1}{R} - \frac{1}{r_{1e}} - \frac{1}{r_{2e}} - \frac{\nabla_R^2}{2\mu} - \frac{\nabla_R^2}{8\mu} \qquad (52)$$

contains all the non-zero diagonal terms. This form is acceptable for calculating the first order correction ψ'. Equation (46) finally becomes:

$$\left\{\langle JM\Lambda|\mathcal{H}^{AD}|JM\Lambda\rangle - E^{AD}\right\}U_{\Lambda} = -\langle JM\Lambda|\mathcal{H} - E^{AD}|JM\Lambda_0\rangle\, U^{AD} \qquad (53)$$

Explicit forms of the operators appearing in (53) are given later. In particular it is shown that the only non-zero matrix elements of the complete Hamiltonian (8) are between states which satisfy the conditions

$$\Lambda = \Lambda_0,\ \Lambda_0 \pm 1 \qquad (54)$$

and for the homonuclear systems there is the further selection rule,

$$u \leftrightarrow u, \quad g \leftrightarrow g, \quad u \not\leftrightarrow g \qquad (55)$$

For the ground electronic state of $HD^{+}(\Sigma_g)$, on which Wolniewicz and Poll have performed their most detailed calculations [58], the only states which are directly coupled nonadiabatically are states of symmetry $\Sigma_g(\Lambda=0)$, $\Sigma_u(\Lambda=0)$, $\Pi_g(\Lambda=\pm1)$ and $\Pi_u(\Lambda=\pm1)$. Each of these is coupled in by a separate term of the complete Hamiltonian so that the second order energy correction may be written as a sum:

$$E'' = E''_{0,g} + E''_{0,u} + 2E''_{+1,g} + 2E''_{+1,u} \qquad (56)$$

where we have used the fact that

$$E''_{+1,g} = E''_{-1,g} \quad \text{and} \quad E''_{+1,u} = E''_{-1,u} \qquad (57)$$

[illegible] easy to write an appropriate expansion for the U_{Λ} by comparison with (25) and (29) for use in (53), as follows:

$$U^{i}_{\Lambda} = R^{-5/2} \sum_{i,j} g_{ij}(\xi,\eta)\chi_{ij}(R) \qquad (58)$$

In this expansion, for Σ_g(j even) and Σ_u(j odd) we have

$$g_{ij}(\xi,\eta) = \exp(-\gamma\xi)(\xi+1)^{\beta}\left[(\xi-1)/(\xi+1)\right]^{i} P^{0}_{j}(\eta) \qquad (59)$$

whilst for Π_g(j odd) and Π_u(j even) we have

$$g_{ij}(\xi,\eta) = (\xi^2-1)^{\frac{1}{2}}\exp(-\gamma\xi)(\xi+1)^{\beta}\left[(\xi-1)/(\xi+1)\right]^{i} P^{1}_{j}(\eta) \qquad (60)$$

The $R^{-5/2}$ term serves to simplify the explicit form of (53). The β and γ are adjustable parameters, determined variationally; with reasonably large expansions (58) the nonadiabatic energy corrections (56) are relatively insensitive to β and γ, and to additional terms in the expansion for U^{i}_{Λ}. The numerical implementation of this approach is described fully by Wolniewicz and Poll [57,58]. For HD^{+} [58] they present nonadiabatic calculations of the energy levels for all bound vibrational states (v=0 to 21) with N=0 to 5, with an estimated accuracy of the order of 0.001 cm^{-1}. Relativistic and radiative corrections were included in these calculations. The results agree well with the available experimental data [45,46], but there do appear to be significant deviations, particularly at higher rotational quantum numbers (see Table 1).

A number of refinements of the calculations could be envisaged. In calculating the nonadiabatic corrections Wolniewicz and Poll neglected the possible effects of the vibration-rotation interaction. The Σ corrections, which are otherwise N independent, were only calculated for N=0; the Π corrections, which are proportional to N(N+1), were only calculated for N=1. Corrections for other N values were obtained by using these results. Wolniewicz and Poll encountered some problems in evaluating the Σ_g correction, related to the difficulty of constructing $\psi(\Sigma_g)$ to be exactly orthogonal

to $\psi^{AD}(\Sigma_g)$ [58]. The use of second ... theory may be inappropriate for considering the Σ_u correction, particularly for high vibrational levels. This is because, as mentioned earlier, the adiabatic potentials for the ground state and first excited state (Σ_u) become identical at very large separations.

(d) Relativistic and radiative corrections.

A detailed treatment of the origin and calculation of these small corrections lies beyond the scope of this review [60-65]. However the corrections are significant and must be included to obtain the most accurate energy levels. The important corrections only involve the motion of the electron and they are diagonal in the adiabatic states, so that they may be introduced as additional terms,

$$\Delta E^r(R) = \langle \phi^{BO} | H^r(R, \underset{\sim}{r}_g) | \phi^{BO} \rangle \qquad (61)$$

to be added to the adiabatic potential (36). The corrections to the adiabatic energy levels are found by obtaining the vibration-rotation eigenvalues for this modified potential. These corrections were included in the nonadiabatic calculations of Bishop and Cheung [55], and of Wolniewicz and Poll [58]. As we seek to perform still more accurate calculations it may be necessary to consider other small corrections, such as the effects of finite nuclear size.

In order to give an indication of the relative sizes of the various corrections we tabulate them for the v=1, N=1 level of HD^+ in Table 2.

In concluding this section we note that the vibration-rotation transition frequencies for HD^+ are sufficiently sensitive to allow a re-determination of the electron/proton mass ratio if the accuracy of both theory and experiment can be improved by an order-of-magnitude [45].

(v) Matrix elements of the Hamiltonian.

In order to apply the formal Hamiltonian (8) to the hydrogen molecular ion we require explicit forms for the operators in terms of the internal coordinates of the system. This is achieved by first separating out the angular motion of the nuclei. and then expressing the resulting matrix elements in terms of the internal coordinates (R, ξ, η). This has been described previously for the two electron systems by Kolos and Wolniewicz [37], but an explicit derivation for the one electron hydrogen molecular ion does not appear to have been given. Attempts to write down the one electron matrix elements from the two electron formulae in [37] appear to have led to some errors in published formulae.

We separate the angular motion of the nuclei by transforming from the space-fixed axes system (X.Y.Z) to a set of rotating molecule-fixed axes. The transformation is defined by two Euler rotations:

(i) ϕ about the initial Z axis $(0 \leq \phi < 2\pi)$

(ii) θ about the resultant y axis $(0 \leq \theta < \pi)$

Following the usual right-handed conventions we obtain the results.

$$\begin{pmatrix} x \\ y \\ z \end{pmatrix} = \begin{pmatrix} \cos\phi\cos\theta & \sin\phi\cos\theta & -\sin\theta \\ \sin\phi & \cos\phi & 0 \\ \cos\phi\sin\theta & \sin\phi\sin\theta & \cos\theta \end{pmatrix} \begin{pmatrix} X \\ Y \\ Z \end{pmatrix} \qquad (62)$$

The coordinates R. θ and ϕ are sufficient to describe the motion of the nuclei.

Applying this transformation. the operator $\underset{\sim}{\nabla}_R$ becomes:

$$\underset{\sim}{\nabla}_R = \left[\cos\phi\sin\theta \left(\frac{\partial}{\partial R}\right)_s + \frac{\cos\phi\cos\theta}{R}\left(\frac{\partial}{\partial\theta}\right)_s - \frac{\sin\phi}{R\sin\theta}\left(\frac{\partial}{\partial\phi}\right)_s\right]\underset{\sim}{i}$$

$$+ \left[\sin\phi\sin\theta \left(\frac{\partial}{\partial R}\right)_s + \frac{\sin\phi\cos\theta}{R}\left(\frac{\partial}{\partial\theta}\right)_s + \frac{\cos\phi}{R\sin\theta}\left(\frac{\partial}{\partial\phi}\right)_s\right]\underset{\sim}{j}$$

$$+ \left[\cos\theta \left(\frac{\partial}{\partial R}\right)_s - \sin\theta \left(\frac{\partial}{\partial\theta}\right)_s\right]\underset{\sim}{k} \qquad (63)$$

where $\underset{\sim}{i}$, $\underset{\sim}{j}$, $\underset{\sim}{k}$ are unit vectors along the space-fixed axes X, Y, Z respectively. The partial differentials in the above operator are to be performed with the electron coordinates in the space-fixed axis system held constant, denoted by the subscript s. The nuclear Laplacian operator becomes:

$$\nabla_R^2 = \frac{1}{R^2}\frac{\partial}{\partial R}\Big)_s\left\{R^2\frac{\partial}{\partial R}\Big)_s\right\} + \frac{1}{R^2}\left[\frac{1}{\sin\theta}\frac{\partial}{\partial\theta}\Big)_s\left\{\sin\theta\frac{\partial}{\partial\theta}\Big)_s\right\} + \frac{1}{\sin^2\theta}\frac{\partial^2}{\partial\phi^2}\Big)_s\right] \quad (64)$$

Use of this form for ∇_R^2 in (34) and (35) allows the rotational motion to be separated; the equations may then be solved numerically as shown, for example, by Cooley [79].

Since the motion of the electron is governed by a molecule-fixed potential,

$$-1/r_{1e} - 1/r_{2e} \quad (65)$$

it is physically more reasonable to transform the operators to a molecule-fixed electron coordinate system, referred to the geometric centre of the internuclear vector. Partial differentials in this coordinate system are denoted by the subscript m. Thus:

$$\begin{aligned}
\frac{\partial}{\partial\phi}\Big)_s &= \frac{\partial}{\partial\phi}\Big)_m + \frac{\partial x}{\partial\phi}\Big)_s\frac{\partial}{\partial x}\Big)_m + \frac{\partial y}{\partial\phi}\Big)_s\frac{\partial}{\partial y}\Big)_m + \frac{\partial z}{\partial\phi}\Big)_s\frac{\partial}{\partial z}\Big)_m \\
&= \frac{\partial}{\partial\phi}\Big)_m - i\cos\theta L_z + i\sin\theta L_x \\
\frac{\partial}{\partial\theta}\Big)_s &= \frac{\partial}{\partial\theta}\Big)_m - iL_y \\
\frac{\partial}{\partial R}\Big)_s &= \frac{\partial}{\partial R}\Big)_m
\end{aligned} \quad (66)$$

The ∇_R^2 operator may now be written as

$$\begin{aligned}
\nabla_R^2 = {} & \frac{\partial^2}{\partial R^2}\Big)_m + \frac{2}{R}\frac{\partial}{\partial R}\Big)_m + \frac{1}{R^2}\left\{\frac{\partial^2}{\partial\theta^2}\Big)_m + \cot\theta\frac{\partial}{\partial\theta}\Big)_m + \frac{1}{\sin^2\theta}\frac{\partial^2}{\partial\phi^2}\Big)_m\right\} \\
& + \frac{1}{R^2}\left\{L_z - L^+L^- - \cot^2\theta L_z^2 - 2i\frac{\cot\theta}{\sin\theta}L_z\frac{\partial}{\partial\phi}\Big)_m\right\} \\
& + \frac{L^+}{R^2}\left\{-\frac{\partial}{\partial\theta}\Big)_m + \frac{i}{\sin\theta}\frac{\partial}{\partial\phi}\Big)_m + \cot\theta L_z\right\} + \frac{L^-}{R^2}\left\{\frac{\partial}{\partial\theta}\Big)_m + \frac{i}{\sin\theta}\frac{\partial}{\partial\phi}\Big)_m + \cot\theta L_z\right\}
\end{aligned} \quad (67)$$

where $L^{\pm} = L_x \pm iL_y$, and L_x, L_y and L_z are the components of the electron angular momentum in the rotating coordinate system. The operator $\nabla_g.\nabla_R$ is treated similarly:

$$\begin{aligned}
\frac{\partial}{\partial X}\Big)_s &= \cos\phi\cos\theta\frac{\partial}{\partial x}\Big)_m - \sin\phi\frac{\partial}{\partial y}\Big)_m + \cos\phi\sin\theta\frac{\partial}{\partial z}\Big)_m \\
\frac{\partial}{\partial Y}\Big)_s &= \sin\phi\cos\theta\frac{\partial}{\partial x}\Big)_m + \cos\phi\frac{\partial}{\partial y}\Big)_m + \sin\phi\sin\theta\frac{\partial}{\partial z}\Big)_m \\
\frac{\partial}{\partial Z}\Big)_s &= -\sin\theta\frac{\partial}{\partial x}\Big)_m + \sin\theta\frac{\partial}{\partial z}\Big)_m
\end{aligned} \quad (68)$$

leading to:

$$\begin{aligned}
\nabla_g.\nabla_R = {} & iP_z\frac{\partial}{\partial R}\Big)_m + \frac{i}{2R}(P^+L^- - P^-L^+) + \frac{iP^+}{2R}\left\{\frac{\partial}{\partial\theta}\Big)_m - \frac{i}{\sin\theta}\frac{\partial}{\partial\phi}\Big)_m - \cot\theta L_z\right\} \\
& + \frac{iP^-}{2R}\left\{\frac{\partial}{\partial\theta}\Big)_m + \frac{i}{\sin\theta}\frac{\partial}{\partial\phi}\Big)_m + \cot\theta L_z\right\}
\end{aligned} \quad (69)$$

where $P^{\pm} = P_x \pm iP_y$, and P_x, P_y and P_z are the components of the electron's impulse operator $\underset{\sim}{P} = -i\nabla_g$ in the molecule-fixed coordinate system. The operators

$$\begin{aligned}
\nabla_g^2 &= \frac{\partial^2}{\partial x^2}\Big)_m + \frac{\partial^2}{\partial y^2}\Big)_m + \frac{\partial}{\partial z^2}\Big)_m \\
V &= \frac{1}{R} - \frac{1}{r_{1e}} - \frac{1}{r_{2e}}
\end{aligned} \quad (70)$$

are both now independent of the Euler angles ϕ and χ.

The forms derived for the operators in the Hamiltonian (8), which can also be found in Kolos and Wolniewicz [37], allow the rotational motion of the molecule to be separated. This is achieved by expanding the total wavefunction as,

$$\psi = \sum_{\Lambda}\Omega^J_{M_J,\Lambda}(\theta,\phi,\chi)U^J_{\Lambda}(\xi,\eta,R) \quad (71)$$

where the functions U^J_{Λ} depend only on the relative positions of the particles, and the $\Omega^J_{M_J,\Lambda}(\theta,\phi,\chi)$ are the normalised symmetric top eigenfunctions

$$\Omega^J_{M_J,\Lambda} = \frac{1}{2\pi}\exp(iM_J\phi)\exp(i\Lambda\chi)d^J_{M_J,\Lambda}(\theta) \quad (72)$$

$\underset{\sim}{J}$ is the total angular momentum in the space-fixed system, M_J is

its component along the space-fixed Z axis, and Λ its component along the molecule-fixed z axis. The motion of the electron about the z axis is described by the angle χ,

$$L_z = -i\frac{\partial}{\partial\chi} \tag{73}$$

The functions $d^J_{M_J,\Lambda}(\theta)$ satisfy the following relations:

$$\left\{\frac{\partial^2}{\partial\theta^2} + \cot\theta\frac{\partial}{\partial\theta} + 2M_J\Lambda\frac{\cot\theta}{\sin\theta} - \frac{M_J^2+\Lambda^2}{\sin^2\theta} + J(J+1)\right\}d^J_{M_J,\Lambda} = 0$$

$$\left\{\frac{\partial}{\partial\theta} - \Lambda\cot\theta + \frac{M_J}{\sin\theta}\right\}d^J_{M_J,\Lambda} = [(J+\Lambda+1)(J-\Lambda)]^{\frac{1}{2}}d^J_{M_J,\Lambda+1}$$

$$\left\{-\frac{\partial}{\partial\theta} - \Lambda\cot\theta + \frac{M_J}{\sin\theta}\right\}d^J_{M_J,\Lambda} = [(J+\Lambda)(J-\Lambda+1)]^{\frac{1}{2}}d^J_{M_J,\Lambda-1} \tag{74}$$

Substituting this form for ψ into the Schrodinger equation (6) leads to the elimination of the Euler angles ϕ and θ, and eventually χ also. Because the Hamiltonian is diagonal in J and M_J we adopt the following designation for its matrix elements:

$$\langle JM_J\Lambda'|\mathcal{H}|JM_J\Lambda\rangle = \langle\Lambda'|\mathcal{H}|\Lambda\rangle \tag{75}$$

From the expressions derived in (67), (69) and (70) for the operators in the Hamiltonian, it is apparent that the only non-zero matrix elements of $\mathcal{H}$ are those which satisfy the Λ selection rule,

$$\Lambda' = \Lambda, \Lambda\pm1 \tag{76}$$

Specifically the non-vanishing matrix elements are as follows:-

$$\langle\Lambda'|\mathcal{H}|\Lambda\rangle = -\frac{1}{2}\langle\Lambda'|\nabla_g^2|\Lambda\rangle + \langle\Lambda'|V|\Lambda\rangle - \frac{1}{8\mu}\langle\Lambda'|\nabla_g^2|\Lambda\rangle - \frac{1}{2\mu}\langle\Lambda'|\nabla_R^2|\Lambda\rangle - \frac{1}{2\mu_a}\langle\Lambda'|\nabla_g\cdot\nabla_R|\Lambda\rangle \tag{77}$$

$$\langle\Lambda'|\nabla_g^2|\Lambda\rangle = 0 \quad \text{unless} \quad \Lambda' = \Lambda \tag{78}$$

$$\langle\Lambda'|V|\Lambda\rangle = 0 \quad \text{unless} \quad \Lambda' = \Lambda \tag{79}$$

$$\langle\Lambda|\nabla_R^2|\Lambda\rangle = \frac{\partial^2}{\partial R^2} + \frac{2}{R}\frac{\partial}{\partial R} - \frac{1}{R^2}\{K(K+1)-\Lambda(\Lambda+1)\} - \frac{1}{R^2}\langle\Lambda|L^+L^-|\Lambda\rangle$$

$$\langle\Lambda-1|\nabla_R^2|\Lambda\rangle = -\frac{1}{R^2}[(J+\Lambda)(J-\Lambda+1)]^{\frac{1}{2}}\langle\Lambda-1|L^-|\Lambda\rangle$$

$$\langle\Lambda+1|\nabla_R^2|\Lambda\rangle = -\frac{1}{R^2}[(J+\Lambda+1)(J-\Lambda)]^{\frac{1}{2}}\langle\Lambda+1|L^+|\Lambda\rangle \tag{80}$$

$$\langle\Lambda|\nabla_g\cdot\nabla_R|\Lambda\rangle = i\left\{P_z\frac{\partial}{\partial R} + \frac{1}{2R}\langle\Lambda|P^+L^- - P^-L^+|\Lambda\rangle\right\}$$

$$\langle\Lambda-1|\nabla_g\cdot\nabla_R|\Lambda\rangle = -\frac{i}{2R}[(J+\Lambda)(J-\Lambda+1)]^{\frac{1}{2}}\langle\Lambda-1|P^-|\Lambda\rangle$$

$$\langle\Lambda+1|\nabla_g\cdot\nabla_R|\Lambda\rangle = \frac{i}{2R}[(J+\Lambda+1)(J-\Lambda)]^{\frac{1}{2}}\langle\Lambda+1|P^+|\Lambda\rangle \tag{81}$$

so that we obtain the results,

$$\langle\Lambda|\mathcal{H}|\Lambda\rangle = -\frac{1}{2}\langle\Lambda|\nabla_g^2|\Lambda\rangle + V - \frac{1}{8\mu}\langle\Lambda|\nabla_g^2|\Lambda\rangle - \frac{1}{2\mu}\left\{\frac{\partial^2}{\partial R^2} + \frac{2}{R}\frac{\partial}{\partial R} - \frac{1}{R^2}[K(K+1)-\Lambda(\Lambda+1)+\langle\Lambda|L^+L^-|\Lambda\rangle]\right\} - \frac{i}{2\mu_a}\left\{P_z\frac{\partial}{\partial R} + \frac{1}{2R}\langle\Lambda|P^+L^- - P^-L^+|\Lambda\rangle\right\}$$

$$\langle\Lambda-1|\mathcal{H}|\Lambda\rangle = [(J+\Lambda)(J-\Lambda+1)]^{\frac{1}{2}}\left\{\frac{1}{2\mu R^2}\langle\Lambda-1|L^-|\Lambda\rangle + \frac{i}{4\mu_a R}\langle\Lambda-1|P^-|\Lambda\rangle\right\}$$

$$\langle\Lambda+1|\mathcal{H}|\Lambda\rangle = [(J+\Lambda+1)(J-\Lambda)]^{\frac{1}{2}}\left\{\frac{1}{2\mu R^2}\langle\Lambda+1|L^+|\Lambda\rangle - \frac{i}{4\mu_a R}\langle\Lambda-1|P^-|\Lambda\rangle\right\} \tag{82}$$

We have now eliminated the Euler angles ϕ and θ from the Hamiltonian by separating the rotational motion of the nuclei. The final stage is to express the above matrix elements in terms of the internal coordinates (R,ξ,η,χ) of the system. This will lead to the elimination of the coordinate χ. We first define some useful operator abbreviations:

$$X = \frac{1}{(\xi^2-\eta^2)}\left\{\frac{\partial}{\partial\xi}(\xi^2-1)\frac{\partial}{\partial\xi} + \frac{\partial}{\partial\eta}(1-\eta^2)\frac{\partial}{\partial\eta}\right\} - \frac{\Lambda^2}{(\xi^2-1)(1-\eta^2)}$$

$$Y = \frac{1}{(\xi^2-\eta^2)}\left\{\xi(\xi^2-1)\frac{\partial}{\partial\xi} + \eta(1-\eta^2)\frac{\partial}{\partial\eta}\right\}$$

$$Z = \frac{1}{(\xi^2-\eta^2)}\left\{\eta(\xi^2-1)\frac{\partial}{\partial\xi} + \xi(1-\eta^2)\frac{\partial}{\partial\eta}\right\}$$

$$A = \frac{[(\xi^2-1)(1-\eta^2)]^{\frac{1}{2}}}{(\xi^2-\eta^2)}\left\{\xi\frac{\partial}{\partial\xi} - \eta\frac{\partial}{\partial\eta}\right\}$$

$$B = \frac{[(\xi^2-1)(1-\eta^2)]^{\frac{1}{2}}}{(\xi^2-\eta^2)}\left\{\eta\frac{\partial}{\partial\xi} - \xi\frac{\partial}{\partial\eta}\right\} \tag{83}$$

The partial derivative $\partial/\partial R$ appearing in the formulae (82) above is performed with the molecule-fixed cartesian coordinates (x,y,z) held constant. With the more useful set of coordinates (ξ,η,χ) held constant we obtain,

$$\left.\frac{\partial}{\partial R}\right|_{xyz} = \left.\frac{\partial}{\partial R}\right|_{\xi\eta\chi} - \frac{Y}{R} \tag{84}$$

Using the results given in the treatment of the Born-Oppenheimer electronic equation, namely (16), (17) and (19), we can write the results:

$$\langle\Lambda|\nabla_g^2|\Lambda\rangle = \frac{4}{R^2}X_\Lambda \tag{85}$$

$$\langle\Lambda|V|\Lambda\rangle = \frac{1}{R} - \frac{4\xi}{R(\xi^2-\eta^2)} \tag{86}$$

$$L^+ = \exp(i\chi)\left\{B + \frac{i\xi\eta}{[(\xi^2-1)(1-\eta^2)]^{\frac{1}{2}}}\frac{\partial}{\partial\chi}\right\}$$

$$\langle\Lambda|L^+|\Lambda\rangle = B - \frac{\xi\eta\Lambda}{[(\xi^2-1)(1-\eta^2)]^{\frac{1}{2}}} \tag{87}$$

$$L^- = \exp(-i\chi)\left\{-B + \frac{i\xi\eta}{[(\xi^2-1)(1-\eta^2)]^{\frac{1}{2}}}\frac{\partial}{\partial\chi}\right\}$$

$$\langle\Lambda-1|L^-|\Lambda\rangle = -B - \frac{\xi\eta\Lambda}{[(\xi^2-1)(1-\eta^2)]^{\frac{1}{2}}} \tag{88}$$

$$P^+ = \frac{2\exp(i\chi)}{R}\left\{-iA + \frac{1}{[(\xi^2-1)(1-\eta^2)]^{\frac{1}{2}}}\frac{\partial}{\partial\chi}\right\}$$

$$\langle\Lambda+1|P^+|\Lambda\rangle = \frac{2i}{R}\left\{-A + \frac{\Lambda}{[(\xi^2-1)(1-\eta^2)]^{\frac{1}{2}}}\right\} \tag{89}$$

$$P^- = \frac{2\exp(-i\chi)}{R}\left\{-iA - \frac{1}{[(\xi^2-1)(1-\eta^2)]^{\frac{1}{2}}}\frac{\partial}{\partial\chi}\right\}$$

$$\langle\Lambda-1|P^-|\Lambda\rangle = \frac{2i}{R}\left\{-A - \frac{\Lambda}{[(\xi^2-1)(1-\eta^2)]^{\frac{1}{2}}}\right\} \tag{90}$$

$$P_z = -\frac{2i}{R}Z \tag{91}$$

With these results we can obtain, after some straightforward manipulations, the matrix elements of the operators appearing in the Hamiltonian (8). They are as follows:-

$$\langle\Lambda|-(\nabla_g^2/2)+V|\Lambda\rangle = \frac{-2X_\Lambda}{R^2} + \frac{1}{R}\left[1 - \frac{4}{(\xi^2-\eta^2)}\right] \tag{92}$$

$$\langle\Lambda|-(\nabla_g^2/8\mu)|\Lambda\rangle = -X_\Lambda/2\mu R^2 \tag{93}$$

$$\langle\Lambda|-(\nabla_R^2/2\mu)|\Lambda\rangle = -\frac{1}{2\mu}\left\{\frac{1}{R^2}\frac{\partial}{\partial R}\left(R^2\frac{\partial}{\partial R}\right) - \frac{2}{R^2}Y\frac{\partial}{\partial R}R + \frac{(\xi^2+\eta^2-1)X_\Lambda}{R^2} - \frac{J(J+1)}{R^2} + \frac{2\Lambda^2}{R^2}\right\} \tag{94}$$

$$\langle\Lambda|-(\nabla_g\cdot\nabla_R/2\mu_a)|\Lambda\rangle = -\frac{1}{\mu_a R^2}\left[Z\frac{\partial}{\partial R}R - \xi\eta X_\Lambda\right] \tag{95}$$

The elements off-diagonal in Λ are:

$$\langle\Lambda-1|-(\nabla_R^2/2\mu)|\Lambda\rangle = \frac{[(J+\Lambda)(J-\Lambda+1)]^{\frac{1}{2}}}{2\mu R^2}\left\{-B - \frac{\xi\eta\Lambda}{[(\xi^2-1)(1-\eta^2)]^{\frac{1}{2}}}\right\}$$

$$\langle\Lambda+1|-(\nabla_R^2/2\mu)|\Lambda\rangle = \frac{[(J+\Lambda+1)(J-\Lambda)]^{\frac{1}{2}}}{2\mu R^2}\left\{B - \frac{\xi\eta\Lambda}{[(\xi^2-1)(1-\eta^2)]^{\frac{1}{2}}}\right\} \tag{96}$$

$$\langle\Lambda-1|-(\nabla_g\cdot\nabla_R/2\mu_a)|\Lambda\rangle = \frac{[(J+\Lambda)(J-\Lambda+1)]^{\frac{1}{2}}}{2\mu_a R^2}\left\{A + \frac{\Lambda}{[(\xi^2-1)(1-\eta^2)]^{\frac{1}{2}}}\right\}$$

$$\langle\Lambda+1|-(\nabla_g\cdot\nabla_R/2\mu_a)|\Lambda\rangle = \frac{[(J+\Lambda+1)(J-\Lambda)]^{\frac{1}{2}}}{2\mu_a R^2}\left\{-A + \frac{\Lambda}{[(\xi^2-1)(1-\eta^2)]^{\frac{1}{2}}}\right\} \tag{97}$$

There is an additional symmetry selection rule on the above matrix elements. The diagonal operator (94) is even in η and so there is the rule,

$$g \leftrightarrow g, \quad u \leftrightarrow u, \quad \text{but} \quad u \not\leftrightarrow g \tag{98}$$

whilst for the odd operator (95) the selection rule is,

$$g \not\leftrightarrow g, \quad u \not\leftrightarrow u, \quad \text{but} \quad u \leftrightarrow g \tag{99}$$

For the operators off-diagonal in Λ, (96) and (97), the matrix elements of the even operator (97) satisfy (99), whilst those of the odd operator (96) obey (98). For the specific case of the ground (Σ_g) state of the hydrogen molecular ion, the matrix element of the adiabatic Hamiltonian, defined by equation (52) is given by the result,

$$\langle {}^1\Sigma_g | \mathcal{H}^{AD} | {}^1\Sigma_g \rangle =$$

$$\frac{-2X_0}{R^2} + \frac{1}{R}\left[1 - \frac{4}{(\xi^2-\eta^2)}\right] - \frac{1}{2\mu_a R^2}\left\{\frac{\partial}{\partial R}\left(R^2\frac{\partial}{\partial R}\right) - 2Y\frac{\partial}{\partial R}R + (\xi^2+\eta^2)X_0 - J(J+1)\right\} \quad (100)$$

Finally the matrix elements of the full Hamiltonian (8) are as follows:-

$$\langle {}^1\Sigma_g | \mathcal{H}^{AD} | {}^1\Sigma_g \rangle =$$

$$\frac{-2X_0}{R^2} + \frac{1}{R}\left[1 - \frac{4}{(\xi^2-\eta^2)}\right] - \frac{1}{2\mu_a R^2}\left\{\frac{\partial}{\partial R}\left(R^2\frac{\partial}{\partial R}\right) - 2Y\frac{\partial}{\partial R}R + (\xi^2+\eta^2)X_0 - J(J+1)\right\} \quad (101)$$

$$\langle {}^1\Sigma_u | \mathcal{H} | {}^1\Sigma_g \rangle = -\frac{1}{\mu_a R^2}\left\{Z\frac{\partial}{\partial R}R - \xi\eta X_0\right\} \quad (102)$$

$$\langle {}^1\Pi_g | \mathcal{H} | {}^1\Sigma_g \rangle = \mp \frac{[J(J+1)]^{\frac{1}{2}}}{2\mu_a R^2} B \quad (103)$$

$$\langle {}^1\Pi_u | \mathcal{H} | {}^1\Sigma_g \rangle = \mp \frac{[J(J+1)]^{\frac{1}{2}}}{2\mu_a R^2} A \quad (104)$$

Matrix elements (101) to (104) are those required for performing nonadiabatic calculations, such as those described by Wolniewicz and Poll [58].

IV. PHOTOELECTRON, PHOTOIONISATION AND PHOTODISSOCIATION SPECTROSCOPY

Prior to 1976 most of the experimental data for the hydrogen molecular ion had been obtained by photoelectron, photoionisation or photodissociation spectroscopy. Other important information was obtained from studies of the Rydberg spectra of H_2 by Takezawa [82] and by Herzberg and Jungen [83], from numerous studies of the electron impact dissociation of H_2 (see, for example, Dunn and Van Zyl [84]), and from investigations of the collision-induced [85] or unimolecular dissociation [86] of H_2^+ and its isotopic modifications. We shall confine our review to experiments

involving photon impact; even so, the techniques discussed in this section are not purely spectroscopic, in that they do not involve direct measurements of the energies of absorbed or emitted photons.

The most extensive information about the vibrational levels of the hydrogen molecular ion has come from photoelectron spectroscopy. In this method a target neutral gas (for example, H_2) is subjected to impact by vacuum-ultraviolet photons, which cause ionisation to produce the molecular ion (H_2^+) in different electronic and vibrational states. The kinetic energies of the ejected electrons are measured and, combined with knowledge of the initial photon energy, provide relative values of the energies of the internal states of the ion. The photoelectron spectrum of molecular hydrogen has been studied by several authors, notably Åsbrink [87], but the most complete and best resolved spectrum has been described recently by Pollard, Trevor, Reutt, Lee and Shirley [88]. The photon source was a helium I_α resonance lamp with an output at 584 Å, and by using a supersonic molecular beam source of n-H_2, p-H_2, HD or D_2, they were able to remove the Doppler broadening. Variation of the molecular beam nozzle stagnation temperature and pressure provided control of the rotational level populations. At a nozzle temperature of 77 K and pressure of 200 torr, the neutral molecules are essentially in the lowest rotational level only; rotational broadening is therefore removed and the vibrational structure of the ions very cleanly resolved, as shown in figure 4. The main results are summarised in Table 3, in which the observed vibrational intervals $\Delta G(v+\frac{1}{2})$ are listed and compared with the best available theoretical values. For H_2^+ and D_2^+ the comparison is with the adiabatic calculations of Hunter, Yau and Pritchard [49], whilst for HD^+ the comparison is with the nonadiabatic calculations of

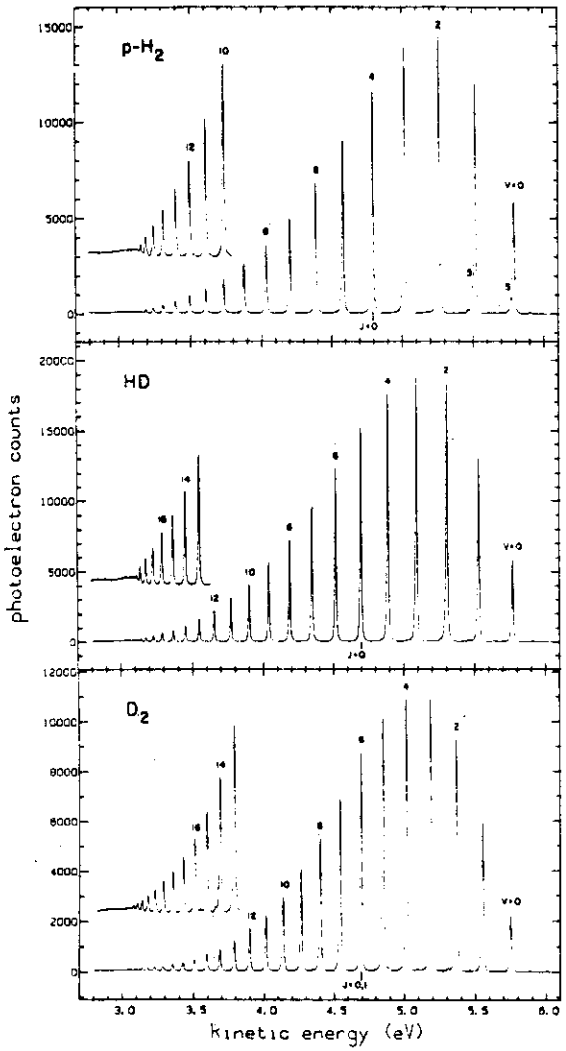

Figure 4

Wolniewicz and Poll [58]. Agreement between experiment and theory is generally very good, but for the highest vibrational levels of H_2^+ and HD^+ the discrepancy seems to be outside the range of experimental error. It remains an open question, therefore, as to whether the nonadiabatic calculations [58], which are excellent for HD^+ in v= 0 to 18, remain good for the final levels, v=19, 20 and 21.

The earlier photoionisation studies of H_2 have now been superceded by the results described above, but they were important at the time of their publication. Following the initial work of Chupka and Berkowitz [89], Peatman [90] described a threshold electron photoionisation study of H_2 in which measurements of the rotational energy levels for v=0 to 7 were obtained. In these experiments (which are closely related to photoelectron spectroscopy) the wavelength of the ionising photons was scanned, but only photoelectrons which had threshold energies of 0 to 3 meV were detected. Consequently the appearance of H_2^+ in different vibration-rotation levels was detected as a function of the photon energy.

Photodissociation studies of H_2^+, D_2^+ and HD^+ have been described by many authors. Following the initial theoretical and experimental work by Dunn [69] and by von Busch and Dunn [70], most investigators have used an accelerated beam of H_2^+ (HD^+, D_2^+) ions, crossed the ion beam with a suitable photon beam, and used a mass filter to separate and collect the photofragment H^+ or D^+ ions. The molecular ions are formed by electron impact on the neutral gas. Because the potential energy curve for the ion is both shallow and displaced to larger internuclear separation, relative to that of the neutral molecule, electron impact ionisation of H_2 in its v=0 level leads to production of H_2^+ in all possible vibrational levels. Franck-Condon factors for the ionising transitions from the ground states

of H_2 and D_2 to all vibrational levels of the ground electronic states of the respective molecular ions have been calculated by a number or workers [36,91,92]. Similar calculations for the production of HD^+ from HD have been described by Tadjeddine and Parlant [71] and, by way of illustration, Table 4 lists the Franck-Condon factors [71] for the production of HD^+ in the lowest rotational level. The vibrational populations should be proportional to these Franck-Condon factors and the use of a collision-free environment, such as an accelerated ion beam, enables the vibrational populations to be conserved. Von Busch and Dunn [70] measured the total photodissociation cross-sections of H_2^+ and D_2^+,

$$H_2^+(1s\sigma_g) + h\nu \longrightarrow H_2^+(2p\sigma_u) \longrightarrow H(1s) + H^+$$

as a function of photon wavelength, using a white light source and a monochromator. In more recent experiments the white light source has been replaced by an argon ion laser operating in the visible. Van Asselt, Maas and Los have described experiments on H_2^+ [72] and HD^+ [93] in which the momentum spectrum of the photofragment H^+ or D^+ ions is recorded. The principles of the experiment are illustrated in Figure 5. The photofragment ions possess excess centre-of-mass kinetic energy, the magnitude of which depends upon the photon energy and the energy of the vibrational level of the molecular ion, relative to the dissociation energy, from which excitation occurs. By using a magnetic analyser to separate the fragment ions from the parent ions, the momentum spectrum of the fragments is obtained. This spectrum yields the relative energies of several different vibrational levels, although the accuracy is rather poor. Of more interest, however, are the fragment ion intensities which depend upon the Franck-Condon factors for ionisation, as discussed above, and also the photodissociation cross-sections for different vibrational levels of the molecular ion.

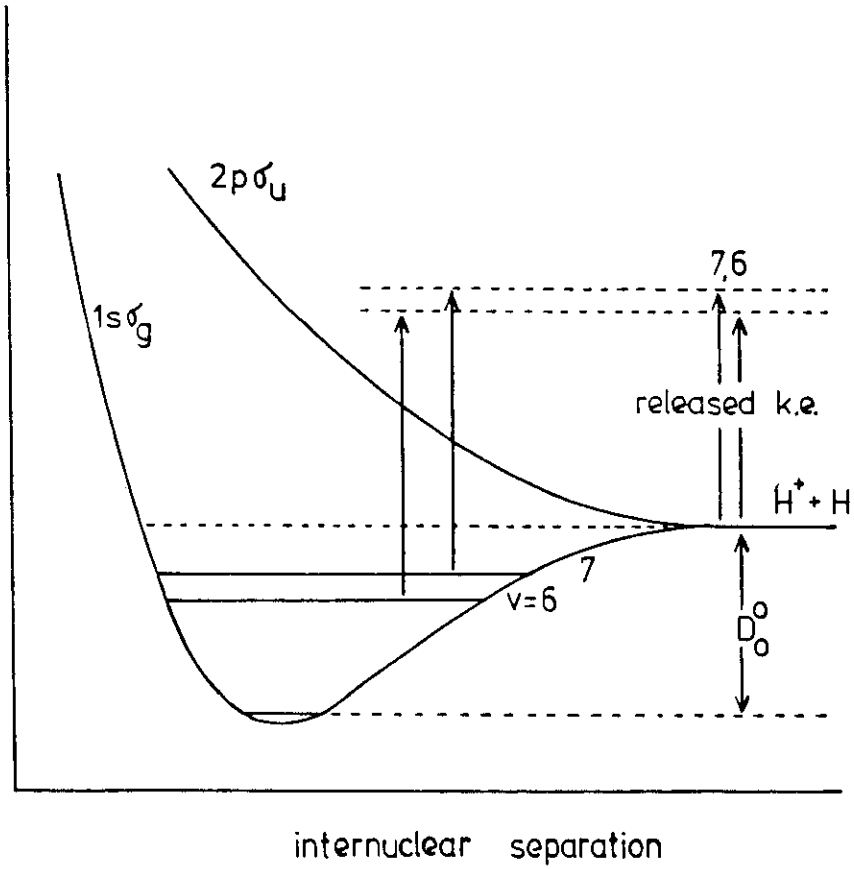

Figure 5

V. RADIOFREQUENCY SPECTROSCOPY

A most ingenious method for obtaining the radiofrequency spectrum of H_2^+ has been described by Dehmelt, Richardson and Jefferts [94,95,96,68]. The method is, in principle, applicable to other ions but it has not yet been extended beyond H_2^+. Before considering the principles and techniques it is helpful to examine qualitatively the hyperfine structure of H_2^+. Figure 6 illustrates the main features. For ortho-H_2^+ the N=1 level, for example, is split into a doublet by the spin-rotation interaction; each level is then further split by nuclear hyperfine interaction as shown. The quantum number J is obtained by adding N and S,

$$\underset{\sim}{J} = \underset{\sim}{N} + \underset{\sim}{S}, \qquad J = N+S,\ N+S-1,\ \ldots,\ |N-S| = 3/2 \text{ or } 1/2$$

and the total angular momentum F is formed by addition of the total nuclear spin I,

$$\underset{\sim}{F} = \underset{\sim}{J} + \underset{\sim}{I}, \qquad F = J+I,\ J+I-1,\ \ldots,\ |J-I| = 5/2,\ 3/2,\ 1/2$$

For para-H_2^+ the net nuclear spin I is zero so that the substructure for N=2 is simpler, as shown. Figure 6 is not necessarily to scale, and we do not wish to presuppose the relative magnitudes of the spin-rotation and nuclear hyperfine interactions.

Dehmelt and Jefferts' experiment is based upon the fact that the photodissociation rates of ions in the ground electronic state are dependent upon F and M_F when the sample is illuminated by linearly polarised light. This is because the photodissociating transition obeys the normal electric dipole selection rules. Consequently a sample of H_2^+ ions held in a collision-free environment and subjected to polarised white light irradiation will develop net spatial alignment because the photodissociation rate is proportional to M_F^2. If, however, transitions between two states F,M_F and F',M_F, are saturated with radiation at the appropriate resonance frequency (which, typically, will be in the radiofrequency

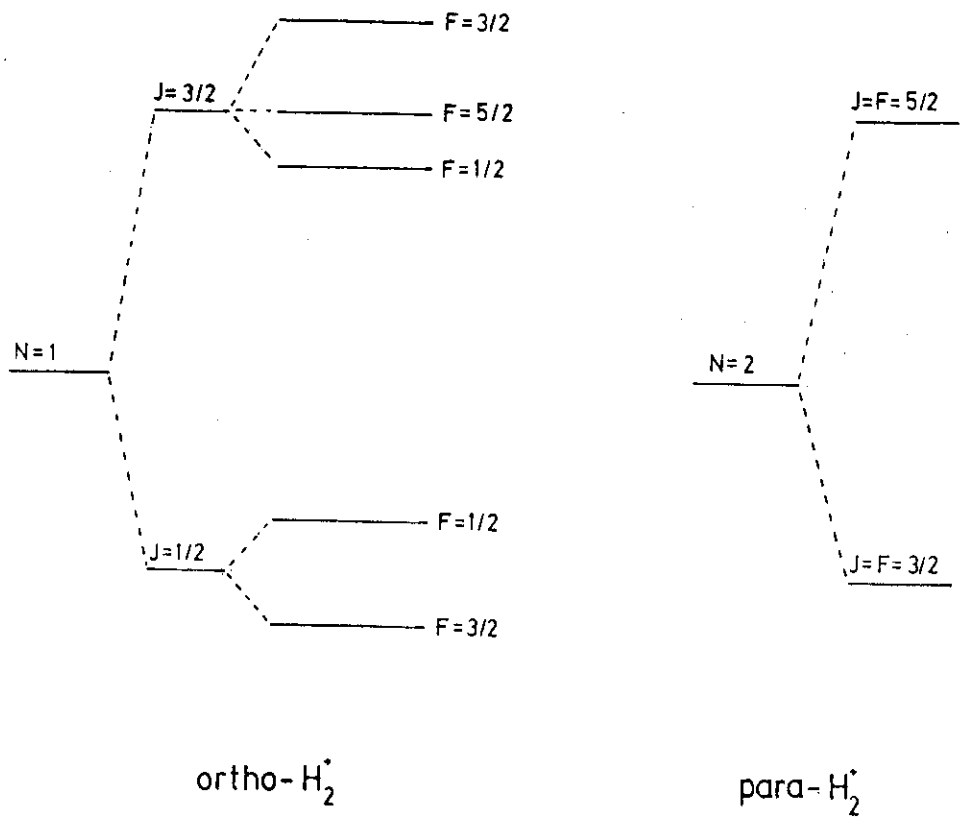

Figure 6

region), the populations become equalised, [illegible] the tendency towards spatial alignment induced by the photodissociation process. Consequently the radiofrequency transitions can be detected by monitoring the net photodissociation rate as a function of the radiofrequency.

In the experiments of Dehmelt and Jefferts the H_2^+ ions are formed in an rf quadrupole ion trap by pulsed electron impact on H_2 at a pressure of 10^{-8} torr. Photodissociation is induced by an intense linearly polarised white light beam providing an average dissociation lifetime of about 30 ms for those ions which can be dissociated by the light. The characteristics of the ion trap allow simultaneous trapping of the H_2^+ and photofragment H^+ ions, and at the end of a suitable irradiation period (for example, 100 ms) the H_2^+ and H^+ ions are extracted, counted, and the ratio H^+/H_2^+ stored in a multichannel digital memory. The frequency of a radiofrequency magnetic field is slowly swept and the transitions detected as changes in the H^+/H_2^+ ratio. The spectroscopic resolution is extremely high because the Doppler width at radiofrequencies is small, and the residence time of the ions in the radiation field is long; line widths in the range 200 to 750 Hz are observed. Figure 7 shows a block diagram of the apparatus used by Jefferts [96]; a small static magnetic field (10 to 30 mG) is used to remove the M_F spatial degeneracy.

The effective Hamiltonian used by Jefferts to interpret his observations was,

$$\mathcal{H}_{eff} = b\underset{\sim}{I}\cdot\underset{\sim}{S} + cI_zS_z + \gamma\underset{\sim}{S}\cdot\underset{\sim}{N} + f\underset{\sim}{I}\cdot\underset{\sim}{N}$$

We shall discuss the form of this Hamiltonian in more detail in the next section. For ions in the v=4 level, for example, the values of the constants were found to be

$b = 804.065$ MHz, $c = 98.034$, $\gamma = 32.636$, $f = 0.038$

Measurements have been made for levels of H_2^+ with v=4 to 8 and

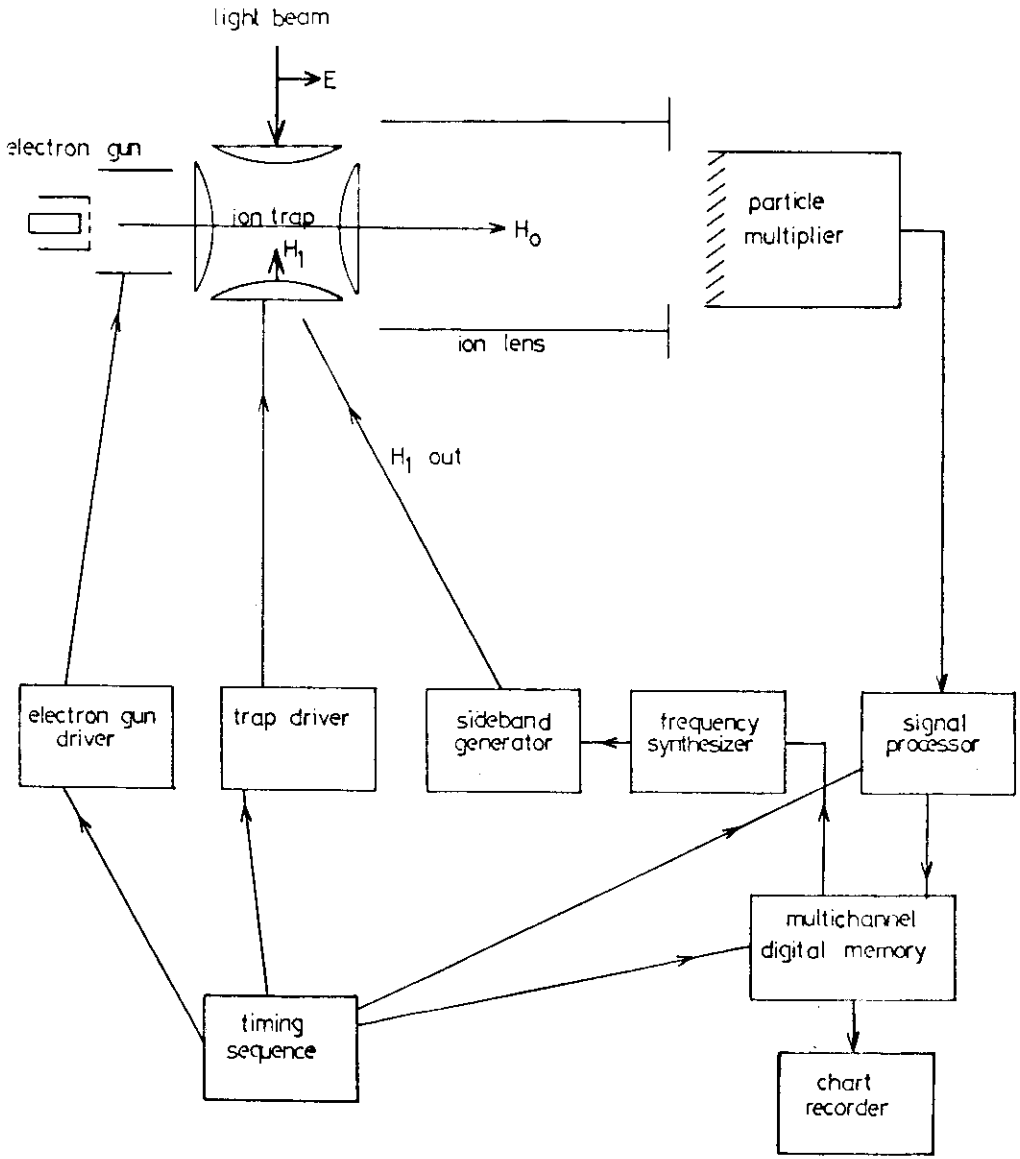

Figure 7

and interpreted by Ray and Certain [67] using the adiabatic potential of Bishop and Wetmore [50]; agreement between theory and experiment is generally very good. Experiments on higher vibrational levels would be desirable, since the nuclear hyperfine and spin-rotation parameters provide excellent tests of the quality of the calculated wavefunctions.

VI. ION BEAM SPECTROSCOPY.

The first infrared spectrum of a gaseous molecular ion was reported in 1976 by Wing, Ruff, Lamb and Spezeski [45] who used the interaction of an infrared CO laser with a beam of HD^+ ions. Subsequently further lines of HD^+ have been observed by the same group [97]. In a related series of experiments Carrington and Buttenshaw [46] and Carrington, Buttenshaw and Kennedy [81] have also observed infrared spectra of HD^+. The transitions observed by Wing et al involve the low vibrational levels, while Carrington et al have observed levels close to the dissociation limits; the experimental methods used by the two groups are different but complementary. The general principle of both methods is that a high velocity, well collimated beam of ions interacts colinearly with one or two infrared laser beams. Changes in the accelerating potential of the ion beam enable vibration-rotation transitions of the ion to be tuned into resonance with a suitable laser line, by means of the Doppler shift. Indirect methods are used to detect population transfer at resonance.

The ions are generally produced by electron impact ionisation of neutral HD, although plasma discharge sources may also be used. The HD^+ ions are extracted by applying a 1 to 10 kV positive potential to the source and are collimated into a narrow beam by a series of electrostatic lenses. The resulting beam possesses a

number of properties offering considerable advantages for spectroscopic study, which we now discuss [98].

(a) Ions present in the beam enjoy a collision-free environment; hence the internal energy distribution of the ions in the beam will reflect directly the energetics of the formation processes in the source. The Franck-Condon factors for ionisation of HD^+, listed in Table 4, show that ions with high vibrational excitation are present in the beam, and this aspect is central to the techniques used by Carrington and his colleagues.

(b) A high degree of spatial control of the ion beam is possible using collimating and deflecting lenses, enabling very efficient interaction with the laser beam to occur.

(c) Unambiguous identification of the ions in the beam can be made through use of the now standard techniques of mass spectrometry. In addition ions of different charge-to-mass ratio can be separated from each other, ion beam intensity measurements are straightforward, and even very weak beams of only a few ions per second can be detected by means of high-gain electron multipliers.

(d) The individual ions in the beam travel at velocities which are typically in the range 10^5 to 10^6 ms^{-1}, depending upon the beam potential and mass of the ion. The effective laser frequency observed by an ion moving at velocity v parallel or antiparallel to the laser beam is given by the relativistic Doppler-shift formula,

$$\nu_{effective} = \nu_{laser} \times \left\{ \frac{1 \pm (v/c)}{1 \mp (v/c)} \right\}^{\frac{1}{2}}$$

where the upper and lower signs refer to antiparallel and parallel orientations respectively, and c is the velocity of light. By sweeping the source potential, frequency

scanning may be achieved with a fixed-frequency laser line.

(e) Sub-Doppler resolution is obtainable as a result of an effect known as kinematic compression or velocity bunching. This effect may be understood [99] by considering two different ions, a and b, of the same mass and which have velocity components in the beam propogation direction,

$$v_a = 0, \qquad v_b = (2kT/m)^{\frac{1}{2}}$$

After acceleration through a potential difference V the ions have final velocity components:

$$v'_a = (2eV/m)^{\frac{1}{2}}$$

$$v'_b = [v_b^2 + (2eV/m)]^{\frac{1}{2}} = (v_b^2 + v'^2_a)^{\frac{1}{2}} = v'_a + \frac{v_b^2}{2v'_a}$$

Hence

$$(v'_b - v'_a)/(v_b - v_a) = \tfrac{1}{2}(kT/eV)^{\frac{1}{2}} = R$$

For T=2000 K and V=10 kV the value of R is 2.1×10^{-3}; consequently the velocity difference and therefore Doppler shift between the different ions is greatly reduced. In practice the resolution is improved by factors of 10 to 100 over normal Doppler-limited spectra as a result of this velocity bunching effect.

Instantaneous ion densities in typical molecular ion beams are estimated to be in the range 10^4 to 10^6 ions/cm^3, which is too low for infrared spectroscopy to be carried out with conventional light sources. Even with the use of high-powered CW lasers it is necessary to use indirect methods to detect the absorption of radiation. Wing and his colleagues have used charge transfer reactions, allowing the HD^+ beam to be partly neutralised with an appropriate target gas after interaction with the laser beam has occurred. The cross-section for charge exchange is dependent upon the vibrational state of the HD^+ ion and therefore the population transfer between vibrational states at resonance with the laser can

be detected by a corresponding change in the degree of charge neutralisation, and hence HD^+ beam intensity.

Carrington and his colleagues have used photodissociation methods, allowing the HD^+ ions to interact with two infrared photons. The first photon is resonant with a vibration-rotation transition through the Doppler effect, whilst the second has sufficient energy to photodissociate the upper level, but insufficient to photodissociate directly the lower level. Resonant population transfer is thus detected as an increase in the number of photofragment H^+ or D^+ ions. It is noteworthy that the resonant signal will be comparable with the background signal in the photodissociation method, whereas in the charge exchange method the change in parent ion beam current after partial neutralisation is relatively small at resonance. The photodissociation method is therefore much the more sensitive, but can only be used to study levels near to the dissociation limit.

The apparatus used by Wing and his group is illustrated in Figure 8. The electron bombardment type source is found to be superior to a plasma discharge source in that it forms ions with less vibrational excitation. Consequently the off-resonance population differences between the initial and final states are greater, enhancing the signal-to-noise ratio. Although the vibrational populations for HD^+ are determined by the Franck-Condon factors for ionisation (Table 4), the rotational distribution is essentially Boltzmann at 320 K. HD^+ ion beam currents of 3×10^{-7} A are produced by admitting a mixture of H_2 and D_2 through a hot palladium leak into the source. After focussing, the ion beam enters a constant potential interaction region, maintained at a pressure of 10^{-6} torr, in which it is crossed at an angle of 11 mrad by an infrared laser beam. The continuous wave CO laser employed is capable of producing 150 lines in the 5.2 to 6.2 μm region. Single line selection is achieved using a diffraction grating and

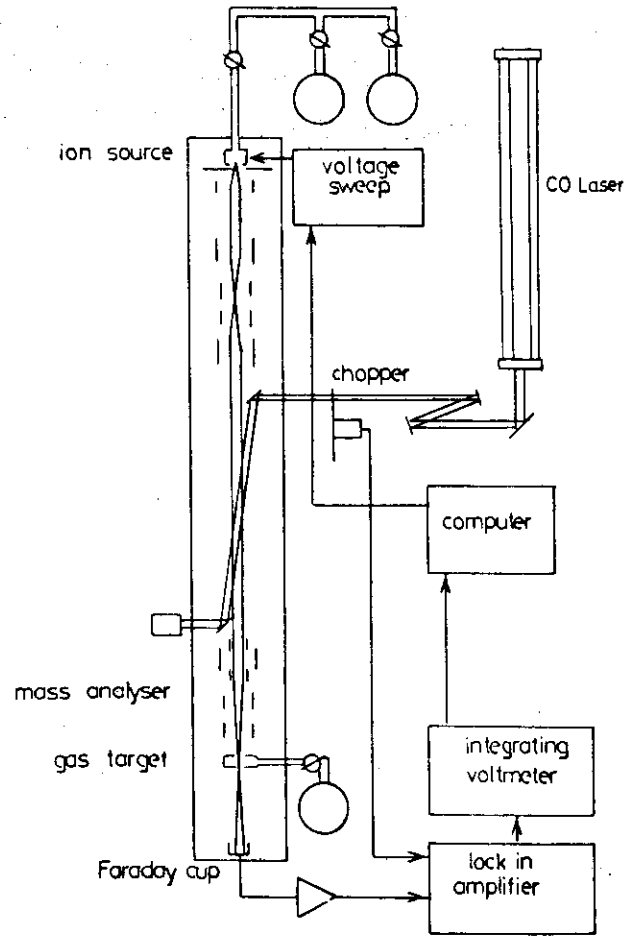

Figure 8

powers of a few mW to 1 W are obtained per line. The source potential is swept by a microcomputer, usually in 0.1 V steps with an integration time of 8 sec per step, in order to Doppler-tune transitions into coincidence with a single selected laser line. After the interaction region, crossed electric and magnetic fields are used to mass-select the HD^+ ions; subsequently the ion current is attenuated by passing the beam through a gas target such as N_2, Ar or H_2, and the remaining ion current is measured at a Faraday cup. The current alters by a few p.p.m. at resonance; hence the laser beam is chopped at 1 kHz and the a.c. Faraday cup signal synchronously detected.

Twenty-five vibration-rotation transitions of HD^+, involving v=0 to 5 and N=0 to 5 have now been observed. All the transitions obey the harmonic oscillator selection rule $\Delta v = \pm 1$, and the measured frequencies are accurate to ± 0.0007 cm^{-1}, the main limitations being voltage calibration and uncertainty in the laser frequencies. The observed linewidths are in the region 7 to 25 MHz, and become smaller at higher source potentials because of increased kinematic compression effects. The experimental results are listed in Table 1; we have already commented on the excellent agreement between experiment and the nonadiabatic calculation [58] for the low vibration-rotation levels. Hyperfine and spin-rotation structure is observed for each line with two or three strong components and one to four weaker components; the splittings range from 12 to 45 MHz, and a satisfactory interpretation has been provided by Ray and Certain [67].

The apparatus employed by Carrington and his colleagues for photodissociation detection of infrared transitions in HD^+ is shown in Figure 9. In essence a tandem mass spectrometer has been adapted for spectroscopic purposes. Ions are formed by electron

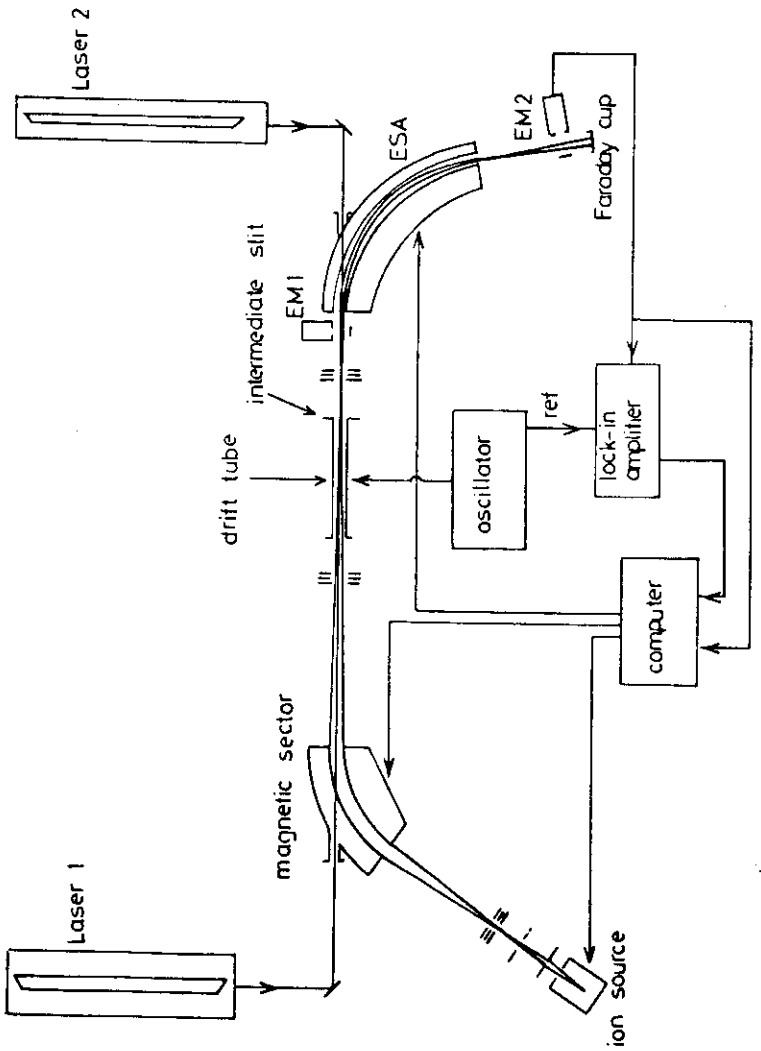

Figure 9

impact or plasma discharge and the extracted ion beam is mass-analysed by a 55° electromagnetic sector. The beam is focussed at the intermediate slit and the ion current may be measured immediately after the slit using an off-axis electron multiplier. The ion beam then passes into an electrostatic analyser (ESA) which selects a particular fragment ion formed from the parent ion between the two analysers. The fragment ion current may be measured either by means of a Faraday cup, or with a second off-axis electron multiplier. Prior to the intermediate slit the ion beam passes through a tube of 40 cm length, known as the drift tube. Potentials in the range -500 to +500 volts may be applied to this tube, and the ESA is able to separate fragment ions formed in the drift tube from those formed elsewhere at earth potential due to their different kinetic energies. The path of the ion beam is evacuated to ~7 x 10^{-8} torr.

Two lasers are available for spectroscopic studies. Laser 1 is of sealed tube design and may be operated with CO as the lasing gas to give maximum powers of 3W in a single line, or with CO_2 giving powers of up to 25W per line. The laser beam is reflected into parallel or antiparallel alignment with the ion beam and is focussed at the intermediate slit. Laser 2 may be operated in a sealed or flowing gas mode with CO_2 as the lasing gas, and has a maximum output power of 60W CW in a single line. The laser beam is aligned antiparallel with the ion beam and focussed into the drift tube, although when both lasers are operated simultaneously a small angle is created between the two laser beams to avoid interference.

In experiments using the photodissociation method both lasers may be used simultaneously. In studies of the v=16-18 band the vibration-rotation transitions are Doppler tuned into resonance with one of the lasers (using CO_2), operated at low power to minimise

power broadening; the transitions are detected by dissociation of the upper state using the other laser (also with CO_2) at high power to maximise the sensitivity. For the v=14-17 band, however, only laser 1 operating with CO is used. Photodissociation occurs mainly from v=17 with the CO laser, and mainly from v=18 with the CO_2 laser.

Several different Doppler tuning and signal detection modes are possible, but for the HD^+ studies the instrument is usually operated in the following manner. A PDP-11 minicomputer is used to scan the source potential over the range 2 to 10 kV, typically in 0.1 to 1 V steps. The magnetic field is simultaneously scanned by the computer to transmit the HD^+ beam at constant intensity. The ESA potential is linked automatically to the source potential, and is set to transmit photoproduct D^+ ions; the computer repeatedly reads the D^+ ion current and adjusts the magnetic sector for maximum intensity. A small d.c. voltage is applied to the drift tube, so that D^+ ions formed in the drift tube may be separated by the ESA from those formed elsewhere; in addition a square-wave modulation of frequency up to 10 kHz and amplitude up to 10 volts is also applied to the drift tube. Voltage modulation causes velocity modulation of the HD^+ beam and is, through the Doppler effect, equivalent to frequency modulation. Hence the ESA voltage is synchronously modulated and a phase-sensitive detector used to demodulate the fragment ion signal; the d.c. signal output is read by the computer for each step of the source potential scan.

The experimental results are listed in Table 1. A total of 9 rotational components of the v=18-16 band, 7 components of the v=17-14 band and 1 component of the v=17-15 band have now been observed. In many cases it is possible to obtain two or three independent measurements of the same transition by using different laser lines, parallel or antiparallel, at different Doppler tuning potentials. Consequently the transition frequencies are determined

to $\pm$ 0.0005 cm^{-1} and, as we have seen in Table 1, the results provide a severe test of the nonadiabatic calculations of Wolniewicz and Poll [58].

Linewidths down to 7 MHz are obtained and each transition shows a doublet splitting, the two lines showing an intensity ratio of about 3 to 1, and separations of from 15 to 25 MHz. This splitting arises from nuclear hyperfine interaction, but it is not immediately obvious why a doublet separation is consistently observed, or what determines the size of the splitting. We must, therefore, consider the effects of the nuclear hyperfine and spin-rotation interactions in more detail. The effective Hamiltonian may be written in the form

$$\mathcal{H}_{eff} = b_1 \underset{\sim}{I}_1 \cdot \underset{\sim}{S} + b_2 \underset{\sim}{I}_2 \cdot \underset{\sim}{S} + c_1 I_{1z} S_z + c_2 I_{2z} S_z + \gamma \underset{\sim}{S} \cdot \underset{\sim}{N}$$

The first two terms represent the Fermi contact interaction between the electron spin ($\underset{\sim}{S}$) and the proton ($\underset{\sim}{I}_1$) and deuteron ($\underset{\sim}{I}_2$) nuclear spins. The third and fourth terms represent the axial components of the dipolar hyperfine couplings, where z is the internuclear axis, whilst the fifth term represents the electron spin-rotation interaction. The simplified form of the dipolar terms implies neglect of non-axial components which have matrix elements connecting different electronic states. We have also neglected the nuclear spin-rotation interaction, and terms describing the deuterium nuclear quadrupole interaction.

Within the restrictions of our Hamiltonian, the hyperfine and fine structure of each vibration-rotation level will depend upon the values of the five constants b_1, b_2, c_1, c_2 and γ. As we saw in section V, information about these constants in H_2^+ has been obtained by Jefferts [96,68] for the levels v=4 to 8. Although extrapolation of these results to the v=16 and 18 levels of HD^+ is undesirably long, they do suggest that the Fermi contact

interaction constant (b_1) for the proton is by far the most important, with a value of approximately 720 MHz. The deuteron constant b_2 would then be expected to be smaller in proportion to the difference in magnetogyric ratios for the proton and deuteron (i.e. by a factor of 0.1535). The dipolar constants c_1 and c_2 are fairly small for the lower vibrational levels and are likely to be even smaller for v=16 and 18. Finally the spin-rotation constant γ is only 32 MHz for v=0 and becomes progressively smaller the higher the vibrational level; we anticipate γ values of only a few MHz for v=16 and higher. These considerations suggest that the most appropriate coupling scheme for the spin and rotational angular momenta is the following:

$$\underset{\sim}{S} + \underset{\sim}{I}_1 = \underset{\sim}{G}_1, \qquad G_1 = 1;0,$$

$$\underset{\sim}{G}_1 + \underset{\sim}{I}_2 = \underset{\sim}{G}_2, \qquad G_2 = 2,1,0;1,$$

$$\underset{\sim}{G}_2 + \underset{\sim}{N} = \underset{\sim}{F}, \qquad F = |N+G_2|, \ldots, |N-G_2|$$

Consequently the hyperfine levels may be characterised by values of the quantum numbers G_1, G_2, N, F and an appropriate energy level diagram for the transition 18,3-16,2 is shown in Figure 10.

The selection rules for the electric-dipole allowed vibration-rotation transitions are $\Delta N = \pm 1$, $\Delta G_1 = \Delta G_2 = 0$, $\Delta F = \pm 1, 0$. The strongest lines therefore arise from the four transitions shown in Figure 10, and any splitting between the lines will arise only from differences in the values of the constants for the two vibrational levels involved. The doublet splittings observed in the HD^+ lines therefore arise primarily from the difference in b_1 for v=16 and 18. The weaker component involves the levels with $G_1=0$, and the stronger component has $G_1=1$. Consequently the stronger component contains unresolved deuterium structure, and each component is probably broadened by unresolved spin-rotation structure. Absolute values of the hyperfine constants could only be obtained through the observation of transitions for which $\Delta G_1 \neq 0$, $\Delta G_2 \neq 0$. Unfortunately

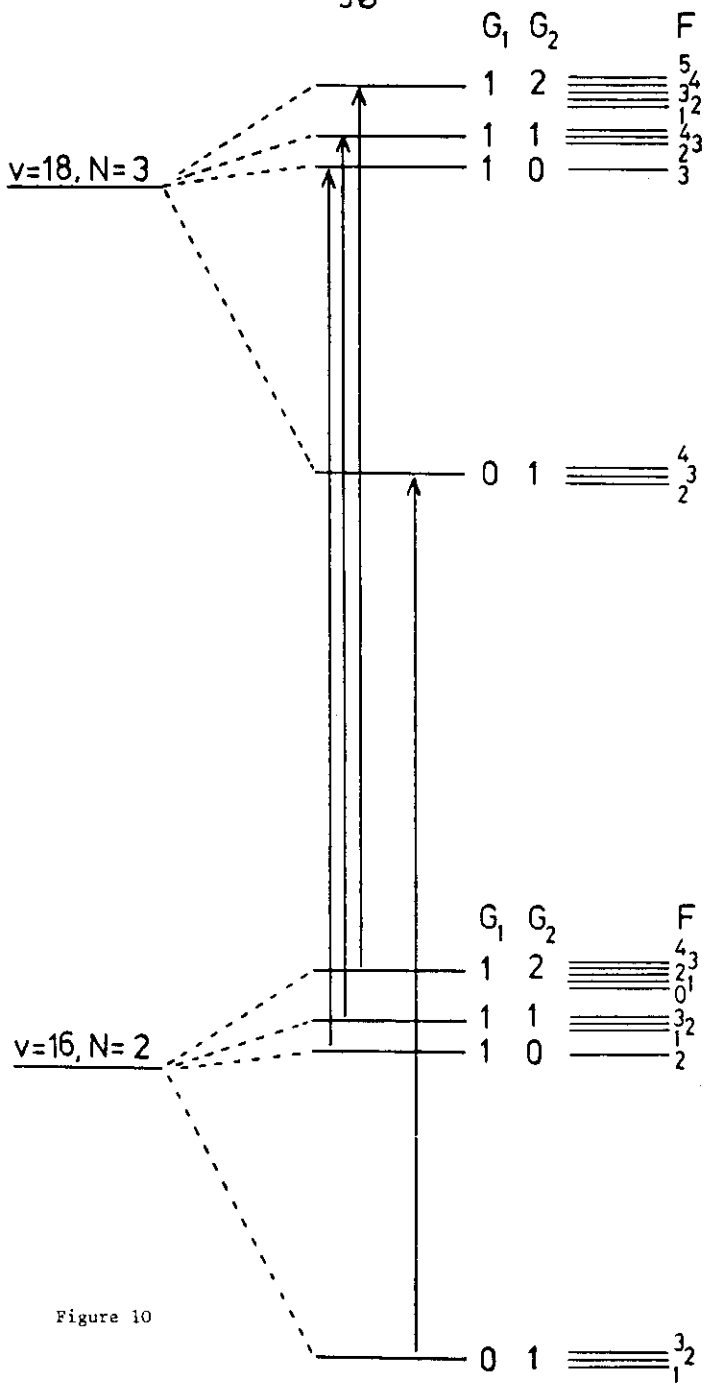

Figure 10

these transitions have very little electric dipole intensity, essentially because the electron spin is only very weakly coupled to the internuclear axis.

The present position for HD^+, therefore, is that experiment and theory agree to within a few thousandths of a wavenumber for levels of moderate v and N value. It may be possible to improve the accuracy of the experiments by an order-of-magnitude, and thus to probe certain more subtle aspects of the molecular physics. The agreement between theory and experiment for the higher vibration-rotation levels is less satisfactory. A particularly challenging experimental problem is to detect transitions involving the highest vibrational levels, v=20 and 21. Searches for such transitions have been made [100], so far without success. The nuclear hyperfine structure for a level which is close to the lower dissociation limit (i.e. within 1 or 2 cm^{-1}) might be most unusual.

Because of the lack of an electric dipole moment in the homonuclear species H_2^+ and D_2^+, vibration-rotation spectra of the type measured for HD^+ are not accessible. It is possible that molecular quadrupole-induced transitions could be detected using the much larger infrared powers available from pulsed sources.

ACKNOWLEDGEMENTS.

A.C. thanks the Royal Society for a Research Professorship and R.A.K. thanks the Science and Engineering Research Council for a Post-Graduate Research Studentship. The ion beam research at Southampton has been supported generously by the SERC, for which we are also grateful.

Table 1. Comparison of experimental transition frequencies for HD^+ with adiabatic and nonadiabatic calculations.

Transition (v',J')-(v",J")	Experiment (cm^{-1})	Adiabatic[e] (cm^{-1})	Nonadiabatic[f] (cm^{-1})	Exp.-Nonadiab. (cm^{-1})
(1,0) - (0,1)	1869.134[a]	1869.25	1869.135	-0.001
(1,1) - (0,2)	1823.533[a]	1823.67	1823.533	0.000
(1,2) - (0,3)	1776.459[b]	1776.60	1776.461	-0.002
(2,1) - (1,0)	1856.778[a]	1856.92	1856.779	-0.001
(3,1) - (2,0)	1761.616[a]	1761.74	1761.616	0.000
(3,2) - (2,1)	1797.522[a]	1797.64	1797.519	0.003
(3,3) - (2,2)	1831.083[b]	1831.21	1831.078	0.005
(3,1) - (2,2)	1642.108[a]	1642.23	1642.111	-0.003
(17,1) - (14,0)	1813.852[c]	1813.66	1813.852	0.000
(17,2) - (14,1)	1820.209[c]	1820.00	1820.201	0.008
(17,3) - (14,2)	1820.199[c]	1819.99	1820.187	0.014
(17,4) - (14,3)	1813.644[c]	1813.43	1813.627	0.017
(17,5) - (14,4)	1800.358[c]	1800.14	1800.333	0.025
(17,6) - (14,5)	1780.145[c]	1779.92	1780.115	0.030
(17,0) - (14,1)	1782.772[c]	1782.57	1782.776	-0.004
(18,1) - (16,0)	926.4895[d]	926.31	926.490	0.000
(18,2) - (16,1)	932.2237[d]	932.03	932.220	0.004
(18,3) - (16,2)	933.2129[d]	933.02	932.207	0.006
(18,4) - (16,3)	929.2471[d]	929.06	929.238	0.009
(18,5) - (16,4)	920.1001[d]	919.91	920.089	0.011
(18,6) - (16,5)	905.5191[d]	905.33	905.512[g]	0.007
(18,7) - (16,6)	885.2183[d]	885.03	885.229[g]	-0.011
(18,0) - (16,1)	901.5648[d]	901.38	901.571	-0.006
(18,1) - (16,2)	882.7312[d]	882.55	882.743	-0.012
(15,7) - (17,8)	1078.8532[d]	1078.67	1078.907[g]	-0.054

[a] from reference [45]

[b] from reference [80]

[c] from reference [81]

[d] from reference [46]

[e] Adiabatic calculations from reference [49]

[f] Nonadiabatic calculations from reference [58]

[g] Extrapolated values, obtained by fitting data of [58] to B, D and H constants.

Table 2. Corrections to the energy of the v=1,J=1 level of HD^+ (in cm^{-1})

Final nonadiabatic energy (rel. to H^++D)	Adiabatic correction*	Nonadiabatic corrections Σ_g	Σ_u	Π_g	Π_u	Relativistic correction [62]	Radiative correction [58]
-19561.222 [58]	~+50	-0.216	-0.038	-0.002	-0.001	-1.572	0.342

*A tabulated value does not seem to be available; this is a crude estimate from the adiabatic potential corrections of Bishop and Wetmore [50].

Table 3. Vibrational differences, $\Delta G(v+\frac{1}{2})$ for H_2^+, D_2^+ and HD^+, measured from the photoelectron spectra (cm^{-1}) [88]. Theoretical values for H_2^+ and D_2^+ from [49], and for HD^+ from [58].

$v+\frac{1}{2}$	H_2^+			D_2^+			HD^+		
	Exp.	Theory	Diff.	Exp.	Theory	Diff.	Exp.	Theory	Diff.
0.5	2190.9	2191.32	-0.42	1583.5	1577.15	6.35	1913.1	1912.994	0.106
1.5	2065.2	2064.09	1.11	1510.0	1512.47	-2.47	1817.2	1816.862	0.338
2.5	1941.8	1941.08	0.72	1450.3	1449.40	0.90	1722.7	1723.587	-0.887
3.5	1822.1	1821.64	0.46	1388.4	1387.81	0.59	1631.8	1632.799	-0.999
4.5	1706.2	1705.13	1.07	1326.3	1327.51	-1.21	1543.0	1544.134	-1.134
5.5	1591.1	1590.90	0.21	1271.0	1268.36	2.64	1456.8	1457.231	-0.431
6.5	1477.7	1478.32	-0.62	1211.2	1210.18	1.02	1372.0	1371.735	0.265
7.5	1367.0	1366.75	0.25	1157.3	1152.83	4.47	1287.5	1287.287	0.213
8.5	1257.8	1255.51	2.29	1091.7	1096.13	-4.43	1201.7	1203.524	-1.824
9.5	1145.8	1143.88	1.92	1044.7	1039.95	4.75	1119.4	1120.066	-0.666
10.5	1031.9	1031.09	0.81	985.8	984.10	1.70	1035.2	1036.522	-1.322
11.5	913.3	916.31	-3.01	927.0	928.41	-1.41	951.3	952.469	-1.169
12.5	796.6	798.59	-1.99	872.7	872.73	-0.03	866.2	867.459	-1.259
13.5	676.4	676.86	-0.46	814.3	816.86	-2.56	779.8	781.002	-1.202
14.5	548.4	549.97	-1.57	759.3	760.60	-1.30	693.2	692.557	0.643
15.5	415.4	416.62	-1.22	702.4	703.77	-1.37	600.6	601.522	-0.922
16.5	280.3	275.96	4.34	644.7	646.12	-1.42	507.2	507.237	-0.037
17.5	-	131.26	-	584.9	587.43	-2.53	409.0	408.975	0.025
18.5	-	-	-	523.9	527.43	-3.53	306.1	306.048	0.052
19.5	-	-	-	463.7	465.84	-2.14	203.0	198.460	4.540
20.5	-	-	-	399.6	402.35	-2.75	-	90.67	-
21.5	-	-	-	327.3	336.63	-9.33	-	-	-
22.5	-	-	-	271.0	268.41	2.59	-	-	-
23.5	-	-	-	-	197.52	-	-	-	-
24.5	-	-	-	-	124.61	-	-	-	-
25.5	-	-	-	-	54.77	-	-	-	-
26.5	-	-	-	-	11.07	-	-	-	-

Table 4. Franck-Condon factors for the ionisation of HD to HD^+, with N=0. Taken from Tadjeddine and Parlant [71]

v	f	v	f	v	f	v	f
0	0.06320	1	0.12862	2	0.15732	3	0.15186
4	0.12845	5	0.10040	6	0.07480	7	0.05416
8	0.03859	9	0.02730	10	0.01928	11	0.01366
12	0.00972	13	0.00696	14	0.00501	15	0.00362
16	0.00261	17	0.00187	18	0.00129	19	0.00083
20	0.00045	21	0.00013				

CAPTIONS TO FIGURES.

Figure 1. Coordinate system for the hydrogen molecular ion. O is the arbitrary space-fixed origin, C.M. is the centre-of-mass of the system and G is the geometric centre of the nuclei.

Figure 2. Cartesian coordinate system.

Figure 3. Born-Oppenheimer potential and adiabatic corrections $H_1 = -\int \phi_s^* (\vec{\nabla}_R^2/2\mu) \phi_s d\tau_g$ and $H_2 = -\int \psi_s^* (\vec{\nabla}_g^2/8\mu) \psi_s d\tau_g$ from the calculations of Bishop and Wetmore [50].

Figure 4. Photoelectron spectra (584 Å) of p-H_2, HD and D_2 expanded from 200 torr at 77 K [88].

Figure 5. Principles of measurement of the momentum of the H^+ ion in the laser photofragmentation of H_2^+.

Figure 6. Hyperfine structure of the N=1 rotational level of ortho-H_2^+, and the N=2 rotational level of para-H_2^+.

Figure 7. Block diagram of the quadrupole trap apparatus used by Jefferts [96].

Figure 8. Ion beam/laser beam apparatus using charge-exchange detection [45].

Figure 9. Tandem ion beam/laser beam apparatus using photodissociation detection [46].

Figure 10. Hyperfine and spin-rotation splitting for the 18,3-16,2 transition in HD^+.

REFERENCES.

[1] T.Oka, Phys.Rev.Letters,45,531(1980).

[2] A.Carrington, J.Buttenshawand N.A.Kennedy, Mol.Phys.45,753(1982)

[3] J.J.Thomson, Phil.Mag.,13,561(1907).

[4] H.C.Urey, Phys.Rev.,27,216 (1926) and references therein.

[5] E.Schrödinger, Ann.Physik.,79,361,489 (1926); 81,109 (1926).

[6] W.Alexandrow, Ann.Physik.,81,603 (1926).

[7] Ø.Burrau, Kgl.Danske Vidensk.Selskal Math.fys.Med.,7,14 (1927).

[8] M.Born and J.R.Oppenheimer, Ann.Physik.,84,457 (1927).

[9] A.Unsöld, Zeits.fur.Physik.,43,563 (1927).

[10] P.M.Morse and E.C.G.Stueckelberg, Phys.Rev.,33,932 (1929).

[11] C.Gilbert, Phil.Mag.,16,929 (1933).

[12] C.A.Coulson, Trans.Faraday Soc.,33,1479 (1937).

[13] E.Teller, Zeits.fur.Physik.,61,458 (1930).

[14] B.N.Dickinson, J.Chem.Phys.,1,317 (1933).

[15] E.U.Condon, Phys.Rev.,35,658 (1930).

[16] W.Bleakney, Phys.Rev.,35,1180 (1930).

[17] W.W.Lozier, Phys.Rev.,36,1285 (1930).

[18] A.H.Wilson, Proc.Roy.Soc.,A118,617,635 (1928).

[19] E.A.Hylleraas, Zeits.fur.Physik.,71,739 (1931).

[20] G.Jaffé, Zeits.fur.Physik.,87,535 (1934).

[21] P.M.Morse, Phys.Rev.,34,57 (1929).

[22] W.W.Lozier, Phys.Rev.,44,575 (1933).

[23] W.G.Baber and H.R.Hassé, Proc.Camb.Phil.Soc.,31,564 (1935).

[24] I.Sandeman, Proc.Roy.Soc.Edinb.,55,72 (1935).

[25] J.L.Dunham, Phys.Rev.,41,713,721 (1932).

[26] O.W.Richardson, Proc.Roy.Soc.,A152,503 (1935).

[27] D.R.Bates, K.Ledsham and A.L.Stewart, Phil.Trans.Roy.Soc., A246,215 (1953).

[28] R.F.Wallis and H.M.Hulbert, J.Chem.Phys.,22,774 (1954).

[29] H.Wind, J.Chem.Phys.,42,2371 (1965).

[30] J.M.Peek, J.Chem.Phys.,43,3004 (1965).

[31] D.R.Bates, J.Chem.Phys.,19,1122 (1951).

[32] A.Dalgarno, T.N.L.Patterson and W.B.Somerville, Proc.Roy.Soc.,A259,100 (1960).

[33] M.J.Stephen and J.P.Auffray, J.Chem.Phys.,31,1329 (1959).

[34] S.Cohen, J.R.Hiskes and R.J.Riddell, Phys.Rev.,119,1025 (1950).

[35] H.Wind, J.Chem.Phys.,43,2956 (1965).

[36] G.H.Dunn, J.Chem.Phys.,44,2592 (1966).

[37] W.Kolos and L.Wolniewicz, Rev.Mod.Phys.,35,473 (1963)

[38] J.H.Van Vleck, J.Chem.Phys.,4,327 (1936).

[39] V.A.Johnson, Phys.Rev.,60,373 (1941).

[40] G.Hunter, B.F.Gray and H.O.Pritchard, J.Chem.Phys.,45,3806(1966)

[41] G.Hunter and H.O.Pritchard, J.Chem.Phys.,46,2146 (1967)

[42] G.Hunter and H.O.Pritchard, J.Chem.Phys.,2153 (1967).

[43] W.Kolos, Adv.Quant.Chem.,5,118 (1970).

[44] D.M.Bishop and L.M.Cheung, Adv.Quant.Chem.,12,1 (1980)

[45] W.H.Wing, G.A.Ruff, W.E.Lamb Jr. and J.J.Spezeski, Phys.Rev.Letters,36,1488 (1976).

[46] A.Carrington and J.Buttenshaw, Mol.Phys.,44,267 (1981).

[47] W.Kolos, Acta.Phys.Acad.Sci.Hungary,27,241 (1969).

[48] C.L.Beckel, E.D.Hansen III and J.M.Peek, J.Chem.Phys.,53, 3681 (1970).

[49] G.Hunter, A.W.Yau and H.O.Pritchard, At.Data Nucl.Data Tables, 14,11 (197- .

[50] D.M.Bishop and R.W.Wetmore, Mol.Phys.,26,145 (1973).

[51] D.M.Bishop, At.Data Nucl.Data Tables,18,521 (1976).

[52] E.A.Colbourn, Chem.Phys.Letters,44,374 (1976).

[53] D.M.Bishop, S.Shih, C.L.Beckel, F.Wu and J.M.Peek, J.Chem.Phys.,63,4836 (1975).

[54] D.M.Bishop, Mol.Phys.,28,1397 (1974).

[55] D.M.Bishop and L.M.Cheung, Phys.Rev.,A16,640 (1977).

[56] E.A.Colbourn and P.R.Bunker, J.Mol.Spectrosc.,63,155 (1976).

[57] L.Wolniewicz and J.D.Poll, J.Mol.Spectrosc.,72,264 (1978).

[58] L.Wolniewicz and J.D.Poll, J.Chem.Phys.,73,6225 (1980).

[59] L.Lathouwers, Phys.Rev.,A18,2150 (1978).

[60] S.K.Luke, G.Hunter, R.P.McEachran and M.Cohen, J.Chem.Phys., 50,1644 (1969).

[61] J.W.Gonsalves and R.E.Moss, Chem.Phys.Letters,62,534 (1979).

[62] D.M.Bishop, J.Chem.Phys.,66,3842 (1977).

[63] J.I.Gersten, J.Chem.Phys.,51,3181 (1969).

[64] D.M.Bishop and L.M.Cheung, J.Phys.,B11,3133 (1978).

[65] D.M.Bishop and L.M.Cheung, J.Chem.Phys.,75,3155 (1981).

[66] R.P.McEachran, C.J.Veenstra and M.Cohen, Chem.Phys.Letters, 59,275 (1978).

[67] R.D.Ray and P.R.Certain, Phys.Rev.Letters,38,824 (1977).

[68] K.B.Jefferts, Phys.Rev.Letters,23,1476 (1969).

[69] G.H.Dunn, Phys.Rev.,172,1 (1968).

[70] F.von Busch and G.H.Dunn, Phys.Rev.,A5,1726 (1972).

[71] M.Tadjeddine and G.Parlant, Mol.Phys.,33,1797 (1977).

[72] N.P.F.B.van Asselt, J.G.Maas and J.Los, Chem.Phys.,11,253(1975).

[73] P.Fournier, B.Lassier-Govers and G.Comtet in "Laser-induced Processes in Molecules", ed. K.L.Kompa (Springer-Verlag), 247 (1979).

[74] P.R.Bunker, Chem.Phys.Letters,27,322 (1974).

[75] D.M.Bishop and L.M.Cheung, Mol.Phys.,36,501 (1978).

[76] J.M.Peek, J.G.Maas and J.Los, Chem.Phys.,8,46 (1975).

[77] J.M.Peek, J.Chem.Phys.,50,4595 (1969).

[78] M.Born and K.Huang, "Dynamical Theory of Crystal Lattices" (Oxford,1954), Appendix VIII.

[79] J.M.Cooley, Math.Comp.,15,363 (1961).

[80] J.J.Spezeski, Ph.D. thesis, University of Yale.

[81] A.Carrington, J.Buttenshaw and R.A.Kennedy, to be published.

[82] S.Takezawa, J.Chem.Phys.,52,2575 (1970); 52,5793 (1970).

[83] G.Herzberg and Ch.Jungen, J.Mol.Spectrosc.,41,425 (1972).

[84] G.H.Dunn and B.Van Zyl, Phys.Rev.,154,40 (1967).

[85] D.K.Gibson and J.Los, Physica,35,258 (1967).

[86] J.G.Maas, N.P.F.B.van Asselt and J.Los, Chem.Phys.,8,37 (1975).

[87] L.Åsbrink, Chem.Phys.Letters,7,549 (1970).

[88] J.E.Pollard, D.J.Trevor, J.E.Reutt, Y.T.Lee and D.A.Shirley, J.Chem.Phys.,77,34 (1982).

[89] W.A.Chupka and J.Berkowitz, J.Chem.Phys.,51,4244 (1969).

[90] W.B.Peatman, J.Chem.Phys.,64,4093 (1976).

[91] D.Villarejo, J.Chem.Phys.,49,2523 (1968).

[92] S.Rothenberg and E.R.Davidson, J.Mol.Spectrosc.,22,1 (1967).

[93] N.P.F.B. van Asselt, J.G.Maas and J.Los, Chem.Phys.Letters, 24,555 (1974).

[94] H.G.Dehmelt and K.B.Jefferts, Phys.Rev.,125,1318 (1962).

[95] C.B.Richardson, K.B.Jefferts and H.G.Dehmelt, Phys.Rev., 165,80 (1968).

[96] K.B.Jefferts, Phys.Rev.Letters,20,39 (1968).

[97] W.H.Wing, private communication.

[98] A.Carrington, Proc.Roy.Soc.,A367,433 (1979).

[99] S.L.Kaufman, Opt.Comm.,17,309 (1976).

[100] A.Carrington and R.A.Kennedy, unpublished work.